

Symmetries in the internal representation of chromaticity

Nicolás Vattuone¹²³⁴, Thomas Wachtler¹² and Inés Samengo³⁴

1. Department of Biology II, Ludwig-Maximilians-Universität München, Germany.

2. Bernstein Center for Computational Neuroscience, Munich, Germany.

3. Department of Medical Physics, Centro Atómico Bariloche, Argentina.

4. Instituto Balseiro, Centro Atómico Bariloche, Argentina.

Abstract

The perceived color of a stimulus depends not only on its spectral properties, but also on those of its surround. For instance, a patch that looks gray on an achromatic surround appears reddish when surrounded by green, and greenish when surrounded by red. Previous studies showed that the effect of the surround is repulsive: It enhances the perceptual difference between stimulus and surround. Here, we performed psychophysical experiments to quantify the repulsion. To report the results, a notion of distance in color space was required. We therefore proposed an individually tailored metric in color space that captured the perceptual abilities of each observer. To define the metric, we determined the minimal chromatic difference between a stimulus and its surround required by each subject to detect the stimulus. Next, observers performed discrimination experiments between two spatially localized stimuli presented on a surround of a different chromaticity. The surround color affected the discrimination thresholds. Quite remarkably, when these thresholds were expressed in the color coordinates defined before, the change in thresholds followed a simple law that only depended on the distance between the surround and the two compared stimuli. Perceptual coordinates, hence, reveal the symmetry of the repulsion effect. This finding was confirmed and modeled with a third experiment, in which subjects were asked to match the color of two stimuli surrounded by two different chromaticities.

1 Introduction

Previous studies have shown that the presence of a chromatic surround modifies the perceived chromaticity of a foreground stimulus (Klauke and Wachtler, 2015, 2016; Kellner and Wachtler,

2016; Wachtler et al., 2001; Ware and Cowan, 1982; Jameson and Hurvich, 1964). For example, a green stimulus appears as yellowish when surrounded by cyan, and as bluish, when surrounded by orange. This effect implies that the function that transforms the activities of S , M and L cones into a higher-level representation of color depends parametrically on the chromaticity of the surround. The perceptual shift is repulsive, since the presence of the surround displaces the perceived foreground color away from that of the surround. It is also non-uniform, since the size of the shift, when reported in any of the color coordinates normally used in colorimetry, varies from place to place in color space. The question remains, however, whether this inhomogeneity could perhaps vanish with an adequate choice of the coordinate system. If such were the case, those privileged coordinates would reveal a fundamental symmetry of the space of colors. In this paper, the ability of an observer to discriminate neighboring colors is used to define a natural system of coordinates individually tailored for the observer in play. In the natural coordinates, the perceptual shift induced by surrounds is approximately homogeneous and isotropic, supporting the hypothesis that the natural coordinates reveal, at least to a good approximation, the properties of the space in which chromatic stimuli are represented internally, and in which contrast-induced computations are performed.

To support these conclusions, here we first find the natural coordinates of each observer by measuring the discrimination thresholds along the S and $L - M$ cardinal directions. We then characterize the way such thresholds are modified by chromatic surrounds, and confirm the homogeneity and isotropy of the effect when reported in the natural coordinates. Finally, we also measure the perceptual shifts produced by surrounds by performing asymmetric matching experiments, in which the colors to be matched are presented against surrounds of different chromaticities. The shifts can be modeled as the consequence of a repulsive field centered at the surround color that, in the natural coordinates, is spherically symmetric.

2 Methods

2.1 Stimuli

Stimuli were displayed on a 21-inch Sony GDM F520 CRT screen, controlled by an ATI Radeon HD 4200 graphics card. The resolution was 1280×1024 pixels, and the refresh rate, 85 Hz. The display was calibrated using a PhotoResearch (Chatsworth, CA) PR-650 spectroradiometer controlled by IRIS software (Kellner and Wachtler, 2016). The coordinates $(\bar{S}, \bar{M}, \bar{L})$ of a

given stimulus were obtained by linearly filtering the measured spectrum with the Stockman and Sharpe (2000) cone fundamentals. A neutral gray was chosen as reference (luminance = 105 cd/m², CIE[x, y] = [0.328, 0.328]), with coordinates $(\bar{S}_g, \bar{M}_g, \bar{L}_g) = (1.48, 40.9, 75.1)$. The cone-contrast coordinates of a stimulus were defined as

$$(S, M, L) = \left(\frac{\bar{S} - \bar{S}_g}{\bar{S}_g}, \frac{\bar{M} - \bar{M}_g}{\bar{M}_g}, \frac{\bar{L} - \bar{L}_g}{\bar{L}_g} \right).$$

These coordinates are invariant under scaling of each of the cone fundamentals. All measurements were performed along the two cardinal chromatic axes (Fig. 1C): the S axis, here noted as x_1 and defined by the condition $L = M = 0$, and the $L - M$ axis (x_2), defined by the conditions $S = 0$ and $L + M = 0$.

The chromatic resolution of each pixel on the screen is limited by the discrete nature of the 8-bit RGB coordinates of the representation of color in the computer, that is, integers between 0 and 255. Varying a single digit by one unit in the RGB representation produces a chromatic change that may be detected by observers in stimuli subtending 2° of the visual field. In order to produce a continuum of chromaticities, and thereby, to design experiments that flexibly approached the threshold discrimination ability of observers, patches were filled with textured colors, constructed as a spatially randomized mixture of pixels colored with four RGB colors of integer coordinates. As neighbouring colors are indistinguishable at the resolution of single pixels, the patches appeared uniform to subjects.

A continuous transformation between the SML and the RGB coordinates can be obtained from the calibration procedure. If the desired stimulus has non-integer RGB coordinates, its four nearest neighbours with integer coordinates, $(RGB)^1, (RGB)^2, (RGB)^3$ and $(RGB)^4$, are used to color the pixels of the stimulus, randomly ordered. The expected fractions (f_1, f_2, f_3, f_4) of pixels appearing with each color are the weights required to produce the desired non-integer RGB color as a convex linear combination, $\sum_i f_i (RGB)^i$ of the four integer neighbors. There is a unique quadruplet of weights that accomplishes this goal. To color each of the 102×102 pixels composing a patch, the index $i \in \{1, 2, 3, 4\}$ labeling each integer neighbour was randomly chosen with probabilities (f_1, f_2, f_3, f_4) .

2.2 Subjects

Seven subjects (4 female, 3 male), aged between 22 and 32 participated in the experiments. Three of them were informed about the purpose of the study, and performed the three exper-

iments. The remaining four were naïve with respect to the study, and performed experiments along a single cardinal axis, either $x_1 = S$ or $x_2 = L - M$, of color space. All observers had normal color vision as assessed by the Farnsworth–Munsell 100 Hue test, and had normal or corrected to normal visual acuity.

2.3 Experimental conditions

The experiments were performed in a darkened room. Subjects were seated, and viewed the display from a distance of about 90 cm. The size of the screen was 40×30 cm, subtending a solid angle of $25^\circ \times 19^\circ$. Subjects were instructed to fix their gaze on a black circle displayed at the center of the screen. Each experiment began with at least 2 min of adaptation to the lighting conditions, during which the subject received instructions and performed test trials that were not included in the analysis. Chromatic stimuli were square patches of 3×3 cm, subtending an angle of approximately 2° .

2.4 Discrimination experiments

A session consisted of 300 trials, lasting for approximately 10 minutes. Throughout a session, the chromaticity b of the surround remained fix and constantly displayed. At the beginning of each trial, a fixation point appeared at the center of the screen, marked by a black circle. After 500 ms, four colored patches were displayed for 150 ms at the cardinal positions (Fig. 1A, B), spanning an angle of 2° between the center of each square and the fixation point. Three of the patches were colored with the so-called *tested* color x , and the fourth, with the *altered* color \tilde{x} , which was different from the other three. The location of the unequal patch was varied randomly from trial to trial among the 4 alternatives. The observer was required to report its position using the keyboard arrows. Subjects had unlimited time to respond. They were allowed to freely set the pace of the experiment by triggering each trial with a key on the keyboard. In each session, the tested color x remained fixed, and the altered color \tilde{x} was chosen randomly among 15 alternatives around x , each sampled 20 times.

In *Experiment I*, the color of the surround coincided with that of the three reference patches (Fig. 1A), so the observer had to detect the location of a single patch on a uniform surround. In *Experiment II*, the surround b had a different chromaticity, so the observer had to compare

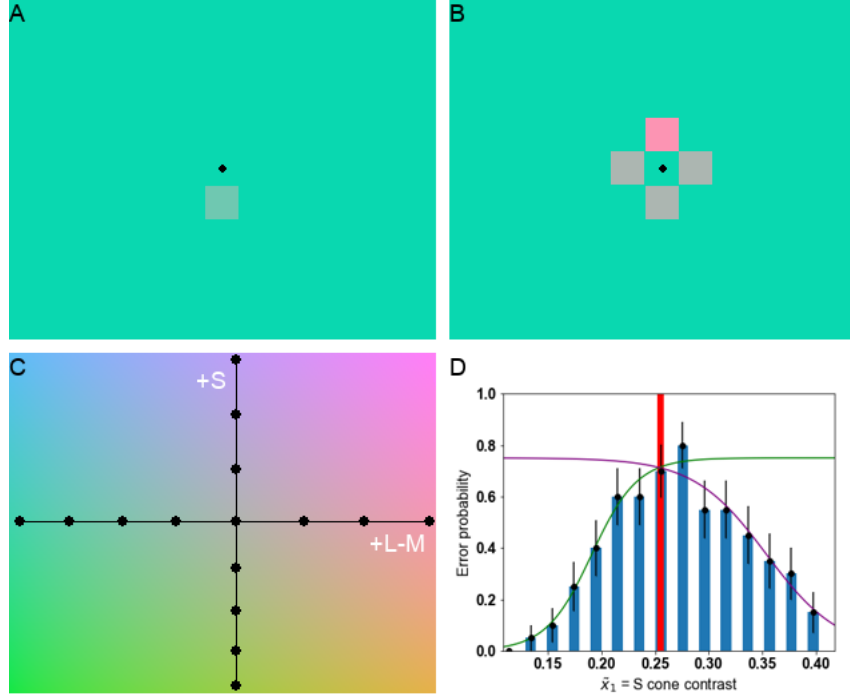


Figure 1: **Experimental paradigms of the discrimination experiments.** Discrimination experiments, performed with surround chromaticity \mathbf{b} equal to (A) or different from (B) the tested color \mathbf{x} . C: Thresholds were measured for eight tested colors on each axis (black circles). The intersection of the axes corresponds to the reference gray. D: Error probability (black bars) reported by subject HW in a session of $N = 20$ trials per target stimulus, as a function of the S cone contrast \tilde{x}_1 of the altered stimulus, for a fixed tested stimulus x_1 (red bar). Random responses are expected to produce 75% of incorrect identifications. As the difference $|\tilde{x}_1 - x_1|$ between the dissimilar patch and the other three increases, the error probability drops. Error bars correspond to the standard error for the binomial distribution for right or wrong choice. The fitted parameters of Eq. 1 are $a_\ell = 0.043 \pm 0.004$, $b_\ell = 0.191 \pm 0.003$, $a_r = 0.07 \pm 0.01$, $b_r = 0.354 \pm 0.006$.

the four patches, and detect the unequal one (Fig. 1B). In both experiments, the color of the surround was varied systematically along the $b_1 = S$ and the $b_2 = L - M$ dimensions, while the total luminosity $L + M$ was maintained constant (Sect. 2.1). In *Experiment I*, each time the surround \mathbf{b} was modified, the tested color \mathbf{x} was changed accordingly. In *Experiment II*, the two colors were varied independently.

As observers select one among four options, when responding randomly, their error rate is 75%. This percentage diminishes as discrimination improves. Figure 1D displays the error probability for subject HW in a given session for different altered colors $\tilde{\mathbf{x}}$ around the tested color \mathbf{x} . We define the discrimination threshold ε from the value of $\tilde{\mathbf{x}}$ for which the error probability is equal to the midpoint between pure chance and perfect performance, i.e. when

the error probability is 37,5%. As reported by Chichilnisky and Wandell (1996), the thresholds may be different for increasing and decreasing cone activation, implying that the bar plot of Fig. 1D need not be symmetric around the maximum. In order to take asymmetries into account, left (ℓ) and right-side (r) thresholds are estimated by fitting a different sigmoid function to each side of the tested color. The fitted functions are

$$P_{\ell,r}(\tilde{x}) = 0.375 [1 \pm \tanh(a_{\ell,r}(\tilde{x} - b_{\ell,r}))], \quad (1)$$

with fitted parameters a_ℓ and b_ℓ or a_r and b_r for the left or right side, respectively. The left (decreasing cone contrast) and right (increasing cone contrast) thresholds of a the reference color x are defined as $\Delta_{\ell r} = |b_{\ell r} - x|$, and the total threshold, as $\varepsilon = \Delta_\ell + \Delta_r$. The expected error of the threshold ε is the sum of the expected errors of the fits of Δ_ℓ and Δ_r .

2.5 Asymmetric matching by forced-choice experiments

Colored surrounds not only modify the discriminability of different stimuli, but also, the mean perceived chromaticity. To assess these changes, subjects performed *Experiment III*: A color matching task in asymmetric conditions. Through a sequence of forced choices (see below), the observer ended up producing a *matched* color that was perceived as chromatically equal to a pre-set *target* color. The asymmetry consisted in performing all comparisons with the target and matched colors surrounded by two different chromaticities. In classical color matching experiments (Commission Internationale de l'Eclairage, 1932; Guild, 1932; Stiles and Burch, 1959; Wyszecki and Stiles, 2000), subjects adjust the matched patch to equalize the target. If no fixation or time constraints are imposed, the results may be contaminated by trial-to-trial variations in the response time, or in the direction of gaze, both of which affect the state of adaptation of visual neurons. To control for these factors, and to work in conditions that are similar to those of the discrimination experiments, we modified the classical asymmetric matching task, transforming it into a sequence of forced choices that iteratively lead to the matched color. In each trial, the observer was presented two candidate patches on one half of the screen surrounded by color b^β , and was instructed to select among them, the one perceived as most similar to a third patch, the target patch, displayed on the other half of the screen, surrounded by color b^α (Fig. 2A). The left/right position of the target patch against b^α and the candidate patches against b^β was randomized in each trial.

Three couples of surrounds were used on each axis. A square patch of chromaticity x^α appeared on surround b^α , giving rise to the combination stimulus $\parallel \text{surround} = x^\alpha \parallel b^\alpha$. The

aim of the task was to iteratively approach the match \mathbf{x}^β on the surround \mathbf{b}^β . In other words, we searched for the color \mathbf{x}^β that fulfilled the perceptual equality $\mathbf{x}^\beta \parallel \mathbf{b}^\beta \sim \mathbf{x}^\alpha \parallel \mathbf{b}^\alpha$. The search for \mathbf{x}^β was structured as a staircase procedure (Sect. 2.5.1). At the beginning of each trial both surrounds were shown for 200 ms, together with a black circle at the fixation point. Then, a patch of color \mathbf{x}^α was presented on \mathbf{b}^α and two patches with colors \mathbf{x}^p and \mathbf{x}^q appeared against the surround \mathbf{b}^β , one above the other (top and bottom locations randomized) for 500 ms. All patches subtended an angle of 2° . A flashing mask appeared next for 500 ms, consisting of randomly sized and located square patches with a balanced distribution of colors along the corresponding axis. Then, the screen turned gray, and the subject was required to respond whether the top or the bottom patch (\mathbf{x}^p or \mathbf{x}^q) was most similar to \mathbf{x}^α . Finally, the fixation point appeared again on the screen, and the subject pressed a key to indicate their readiness to initiate the next trial. The masking and the gray screen were introduced to mitigate after-image effects and to control the adaptation state of the eye.

2.5.1 Staircase procedure

In each trial, two patches with colors \mathbf{x}^p and \mathbf{x}^q appeared on the surround \mathbf{b}^β . The subject was requested to select the one that appeared to be most similar to the target \mathbf{x}^α , presented against the surround \mathbf{b}^α . If they were not able to decide, they were instructed to respond randomly. The two options \mathbf{x}^p and \mathbf{x}^q constituted upper and lower bounds for the matched color \mathbf{x}^β , and were updated progressively throughout the $n = 6$ steps conforming a trial. In the first step of the procedure, \mathbf{x}_1^p and \mathbf{x}_1^q took the maximal and minimal values allowed by the display for the corresponding axis. For instance, along the $x_1 = S$ axis, initially \mathbf{x}_1^p was a maximally saturated purple and \mathbf{x}_1^q , a maximally saturated yellow-green. At step i , the subject decided whether $\mathbf{x}_i^p \parallel \mathbf{b}^\beta$ or $\mathbf{x}_i^q \parallel \mathbf{b}^\beta$ was perceived as more similar to $\mathbf{x}^\alpha \parallel \mathbf{b}^\alpha$. For the step $i + 1$, the non-selected bound at step i was updated by the midpoint between the two previous options, that is,

$$\begin{aligned}\mathbf{x}_{i+1}^p &= \mathbf{x}_i^p + z_i \frac{\mathbf{x}_i^p - \mathbf{x}_i^q}{2} \\ \mathbf{x}_{i+1}^q &= \mathbf{x}_i^q - (1 - z_i) \frac{\mathbf{x}_i^p - \mathbf{x}_i^q}{2}\end{aligned}$$

where $z_i = 0$ if the subject chose \mathbf{x}_i^p , and $z_i = 1$, otherwise. Both sequences were bounded and monotonic, and their distance decreased exponentially, so they both converged to the same value \mathbf{x}^β . We estimated this value as $(\mathbf{x}_6^p + \mathbf{x}_6^q)/2$, and interpreted as the color for which $\mathbf{x}^\beta \parallel \mathbf{b}^\beta$ matched $\mathbf{x}^\alpha \parallel \mathbf{b}^\alpha$. We verified that after 6 steps, the two bounds were indistinguishable.

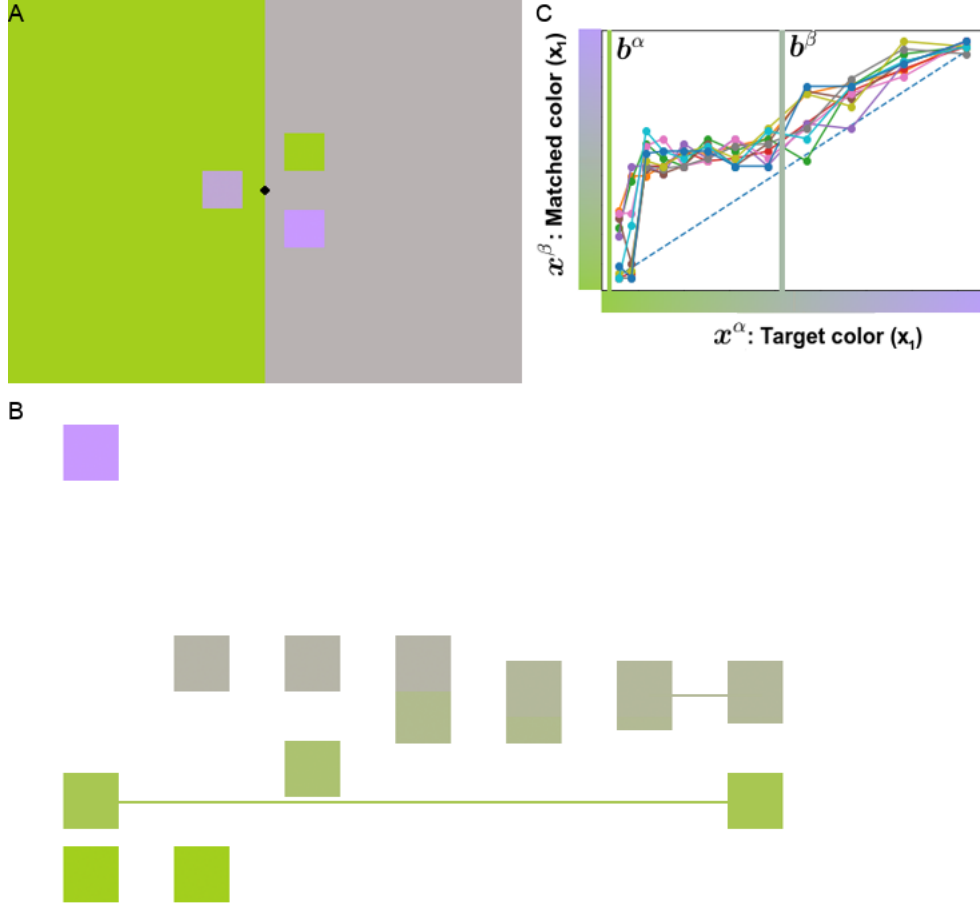


Figure 2: **Experimental paradigms of the similarity experiments.** A: Two patches x^p and x^q are presented on the right, surrounded by color b^β . The observer must report the one perceived as most similar to the target stimulus x^α on the left, which is surrounded by color b^α . B: Sequence of chromaticities x^p and x^q appearing in response to the choices of the subject. Horizontal axis: trial number. Vertical axis: coordinate $S = x_1$ of each patch. Horizontal line: target color x^α . The trial contains 6 iterations, after which the final matched stimulus x^β is calculated as the average of the reached x_6^p and x_6^q . C: Color x^β presented on surround x^β (gray line) that matches the color x^α when presented on surround b^α (green line). Different lines represent each of the 10 trials responded by observer HW.

2.6 The natural coordinates

Discrimination thresholds can be understood as the granularity with which the space of colors is perceived. The core idea is that two colors separated in less than the threshold are not reliably represented as different in the brain area or areas employed to decide whether they are different or not. Yet, the size of thresholds, and their variation throughout color space, depend on the coordinate system. In this paper, we report the experimental results in the cone contrast

coordinates $x_1 = S$ and $x_2 = L - M$ (Derrington et al., 1984), maintaining the total luminosity $x_3 = L + M$ fixed, as done in previous studies Klauke and Wachtler (2015). Each color is represented as a column vector \mathbf{x} with components x_1 and x_2 . In order to reveal the symmetries of color space, we use the measured thresholds to define the so-called *natural coordinates* (x'_1, x'_2) of each observer, in which all discrimination thresholds are uniform and isotropic. To transform from the cone contrasts to the natural coordinates we develop a procedure based of a notion of distance in color space that encompasses the granularity defined by the measured thresholds. The proposed distance is derived from a metric tensor, as explained in this section.

If $J(\mathbf{x})$ is the metric tensor of the space of colors, the line element $d\ell$ measuring the distance between a given color \mathbf{x} and the infinitesimally displaced color $\mathbf{x} + d\mathbf{x}$ is

$$\begin{aligned} d\ell &= \text{Dist}(\mathbf{x}, \mathbf{x} + d\mathbf{x}) \\ &= \sqrt{d\mathbf{x}^t J(\mathbf{x}) d\mathbf{x}} \\ &= \sqrt{J(\mathbf{x})_{11} (dx_1)^2 + 2 J(\mathbf{x})_{12} dx_1 dx_2 + J(\mathbf{x})_{22} (dx_2)^2}, \end{aligned} \tag{2}$$

where the suprascript t represents vector transposition, and $J(\mathbf{x})$ is the symmetric and non-negative tensor that encompasses the chosen notion of distance. Our aim is to find the tensor $J(\mathbf{x})$ that represents perceptual differences, that is, the one for which the distance $d\ell$ between two neighboring colors \mathbf{x} and $\mathbf{x} + d\mathbf{x}$ captures their behavioral discriminability. If an observer is capable of particularly accurate discrimination between \mathbf{x} and a slightly displaced color along a direction \hat{e} , the discrimination threshold must be particularly small in this direction. The smaller the threshold, the more sensitive the observer. It therefore makes sense to define perceptual distances inversely proportional to discrimination thresholds.

To construct $J(\mathbf{x})$, the discrimination threshold between color \mathbf{x} and a displaced color along the direction \hat{e} needs to be measured for every possible direction \hat{e} . Operationally, this means to move progressively away from \mathbf{x} , in small steps that add up to ε , along the direction \hat{e} , and to test whether the reached color $\mathbf{x} + \varepsilon \hat{e}$ can be discriminated from \mathbf{x} with a pre-set accuracy. If the reached color passes the test, then \mathbf{x} and $\mathbf{x} + \varepsilon \hat{e}$ are defined to be at a fixed distance from each other. In this paper, we define the units of length by setting this distance as equal to 1: A length of one unit in color space is equal to a pre-set discrimination accuracy (see Sect. 2.4, where the threshold accuracy is defined). If the reached color cannot be discriminated from \mathbf{x} , the size of ε is increased, and the procedure is iterated until the first color that passes the test is reached.

If thresholds are assumed to vary continuously with the direction \hat{e} , the lowest-order analyt-

ical expression that captures their directional modulation is given by the equation of an ellipse. That is, the vector $(\varepsilon \hat{e})^t = (\varepsilon_1, \varepsilon_2)$ is a solution of

$$(\varepsilon \hat{x})^t E(\mathbf{x}) \varepsilon \hat{x} = (\varepsilon_1, \varepsilon_2) \begin{pmatrix} E_{11}(\mathbf{x}) & E_{12}(\mathbf{x}) \\ E_{21}(\mathbf{x}) & E_{22}(\mathbf{x}) \end{pmatrix} \begin{pmatrix} \varepsilon_1 \\ \varepsilon_2 \end{pmatrix} = 1,$$

where $E(\mathbf{x})$ is the symmetric non-negative matrix with entries $E_{ij}(\mathbf{x})$ representing the quadratic form of the elliptic thresholds. The eigenvectors of $E(\mathbf{x})$ are aligned with the principal axes of the ellipse, and the eigenvalues are the square of their lengths. The inverse relation between thresholds and distances implies that

$$J(\mathbf{x}) = E(\mathbf{x})^{-1}. \quad (3)$$

Equation 3 defines the metric tensor with which infinitesimal displacements can be measured through Eq. 2. The length of a path connecting two remote colors is obtained by integrating local increments along the trajectory. Conceptually, this means that the total length is the number of thresholds that need to be crossed to travel from one color to the other. Of course, the metric tensor may change along the way, and different paths may have different lengths. The distance is then defined as the length of the shortest path. For practical reasons, $J(\mathbf{x})$ cannot be estimated for the infinite collection of points \mathbf{x} composing the trajectory. In order to calculate the path integral, hence, $J(\mathbf{x})$ must be estimated for a subset of colors \mathbf{x} that sample the curve under study with sufficient resolution. The intermediate tensors are then interpolated under the assumption that the discrimination ability varies continuously between samples.

Krauskopf and Gegenfurtner (1992) have shown that, in the cone contrast coordinates, the diagonal terms of $J(\mathbf{x})$ vanish. In this case, thresholds only need to be measured along the cardinal axes e^1 and e^2 . Infinitesimal distances along the axes then read

$$\begin{aligned} d\ell_i &= \text{Dist} [\mathbf{x}, \mathbf{x} + dx_i e^i] \\ &= \sqrt{J_{ii}(\mathbf{x}) (dx_i)^2} \\ &= \frac{|dx_i|}{\varepsilon(e^i)}, \end{aligned} \quad (4)$$

where the subscript i indicates either the S ($i = 1$) or the $L - M$ ($i = 2$) coordinate. The distance between two colors \mathbf{x}^a and $\mathbf{x}^b = \mathbf{x}^a + \Delta e^i$ that differ in a vector aligned with the cardinal axes i , but are not necessarily near, is found by integration

$$\begin{aligned} \text{Dist} [\mathbf{x}^a, \mathbf{x}^b] &= \int_{\mathbf{x}^a}^{\mathbf{x}^b} d\ell \\ &= \int_{\mathbf{x}^a}^{\mathbf{x}^b} \sqrt{J_{ii}(\mathbf{x})} |dx_i| \end{aligned} \quad (5)$$

If $J(\mathbf{x})$ is diagonal, and in addition, the term $J_{ii}(\mathbf{x})$ only depends on the component x_i , the space of colors has zero curvature. In this case, a coordinate transformation $\mathbf{x} \rightarrow \mathbf{x}'$ exists, such that the transformed metric is Euclidean. In Euclidean spaces, all geodesics are straight lines, which greatly simplifies the perceptual shift produced by surrounds, as explained below. In the new coordinates, the discrimination ability of the observer is isotropic and homogeneous, that is, all ellipsoids are turned into spheres, and all spheres have the same size. These are the coordinates that most naturally reveal the perceptual abilities of the subject, and are therefore here called the *natural* coordinates of the observer. It is easy to prove that the function instantiating the transformation to the natural coordinates is

$$\begin{aligned} x'_1(\mathbf{x}) &= d[(x_1^0, x_2^0)^t, (x_1, x_2)^t] \\ &= \int_{x_1^0}^{x_1} \sqrt{J(y_1, x_2^0)} \, dy_1, \end{aligned} \quad (6)$$

$$\begin{aligned} x'_2(\mathbf{x}) &= d[(x_1^0, x_2^0)^t, (x_1^0, x_2)^t] \\ &= \int_{x_2^0}^{x_2} \sqrt{J(x_1^0, y_2)} \, dy_2, \end{aligned} \quad (7)$$

where $d(\mathbf{x}^p, \mathbf{x}^q)$ is the distance between colors \mathbf{x}^p and \mathbf{x}^q , and \mathbf{x}^0 is the origin of the new system of coordinates ($\mathbf{x}'(\mathbf{x}^0) = \mathbf{0}$) and may be chosen arbitrarily.

3 Results

3.1 Classes of equivalence in the space of stimuli \times surrounds

The chromatic shift produced by surrounds hints to the possibility that there be no such thing as the chromaticity of a stimulus as such, independent of its surround, or more generally, independent of the context in which the stimulus is viewed. For definiteness, in this paper we study the effect of chromatic surrounds, other contextual variables remaining fixed. The starting point is the assumption that the color with which a stimulus is perceived depends on the spectral properties of both the stimulus and the surround. Mathematically, this means that

$$\text{Perceived color} = \text{Function}[\mathbf{x}^{\text{stim}}, \mathbf{x}^{\text{sur}}], \quad (8)$$

where \mathbf{x}^{stim} and \mathbf{x}^{sur} represent the stimulus and the surround, respectively. In trichromats, three numbers suffice to characterize the perceivable properties of the power spectrum, giving rise to the well-known 3-dimensional color spaces, such as *LMS*, *RGB*, *XYZ*, or others. Equation 8

implies that, in order to specify a percept, 6 coordinates are required, 3 for the color of the stimulus and 3 for the surround.

Yet, quite remarkably, observers engage themselves naturally in asymmetric matching experiments, where they are asked to match pairs of stimuli surrounded by different colors. The feasibility of the task implies that surrounds do not induce a novel percept, shifting the stimulus along new dimensions that have nothing to do with color. They rather shift the sensation of color to some other nearby sensation, which is a percept of the same type, i.e., it belongs to the same space. More technically, surrounds modify the mapping between the spectral properties of the stimulus x and the internal representation of color. Were it not so, observers would question the whole asymmetric matching task, refusing to pair stimuli that are perceived as different in nature, as they would surely do if asked to match a color with an odor. This idea is here formalized by the assumption that for each stimulus x^α presented against surround b^α , and for each new surround b^β , a new stimulus x^β can be defined by a function

$$x^\beta = \Phi_{b^\alpha \rightarrow b^\beta}(x^\alpha), \quad (9)$$

such that

$$x^\alpha \parallel b^\alpha \sim x^\beta \parallel b^\beta. \quad (10)$$

In Eq. 10, the symbol “ \sim ” means that stimulus x^α surrounded by b^α appears to have the same chromaticity as stimulus x^β surrounded by b^β .

In asymmetric matching experiments, observers compute the function $\Phi_{b^\alpha \rightarrow b^\beta}$. As first noted by Resnikoff (1974), the matching operation “ \sim ” defines an equivalence relation, that is, a relation between pairs of “stimulus \parallel surround” that is reflexive ($x \parallel b \sim x \parallel b$), symmetric (if $x^\alpha \parallel b^\alpha \sim x^\beta \parallel b^\beta$ then $x^\beta \parallel b^\beta \sim x^\alpha \parallel b^\alpha$), and transitive (if $x^\alpha \parallel b^\alpha \sim x^\beta \parallel b^\beta$ and also $x^\beta \parallel b^\beta \sim x^\gamma \parallel b^\gamma$, then $x^\alpha \parallel b^\alpha \sim x^\gamma \parallel b^\gamma$). All equivalence relations induce a partition in the set they operate upon. In other words, the set of pairs $x \parallel b$ can be segmented into disjoint subsets, or *classes of equivalence*. All pairs belonging to the same class are pairwise connected with the relation \sim , and also, pairs belonging to different classes are not connected with \sim . In line with Resnikoff, here we assume that a given *color*, or equivalently, a given *chromaticity*, is the percept shared by all the pairs that belong to the same class. Color is therefore not a property of a specific stimulus x , nor even of a specific pair $x \parallel b$. It is a property of a whole class of pairs. In mathematical terms, color is defined in the quotient space defined by the classes of equivalence. Therefore, the 6 coordinates mentioned above are redundant, since pairs belonging to the same class of equivalence are symbolized with different numbers. Classes of equivalence are 3-dimensional submanifolds embedded in the 6-dimensional space defined

by stimuli and surrounds. If selecting a color is equivalent to selecting a class, 3 coordinates suffice. In Fig. 3, the classes of equivalence are illustrated for four different choices for the function defining the displacements induced by surrounds. Since it is not possible to depict 3-dimensional submanifolds embedded inside a 6-dimensional space, the figure shows slices containing the axes (x_1, b_1) and (x_2, b_2) , respectively. In these slices, each class appears as a curve. In Fig. 3A, the surround does not alter the perceived color of the stimulus, and therefore,

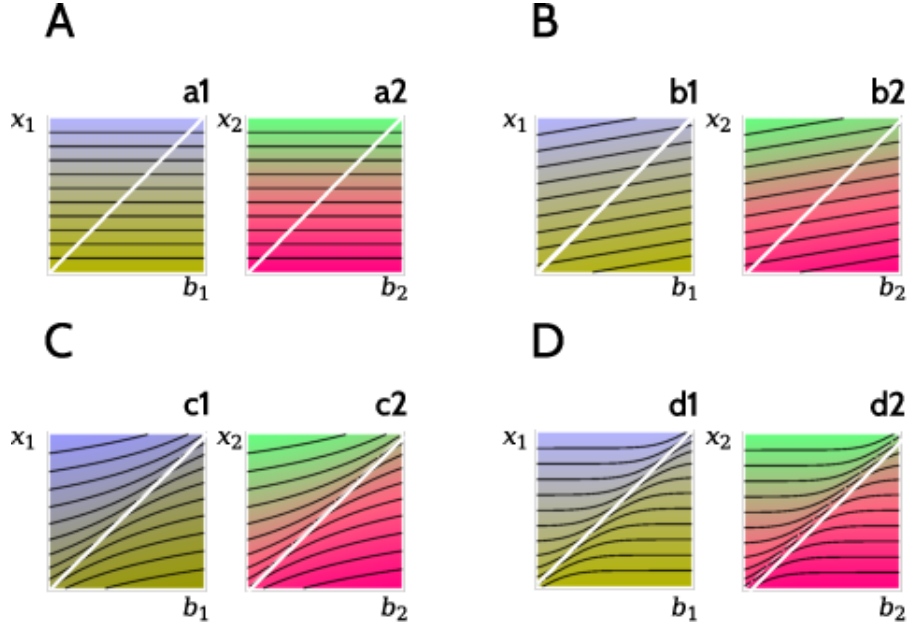


Figure 3: **Classes of equivalence.** Four different examples of the structure of the partition induced by classes of equivalence. Black lines represent classes of equivalence, and are obtained by plotting $\Phi_b(x)$ for fixed x (one value per line) and varying b . The diagonal white line contains the uniform representatives. **A:** The surround does not alter the color of the stimulus, so the classes of equivalence are planar (straight lines). **B:** The surround induces a linear classes of equivalence, as suggested by Resnikoff (1974) and Provenzi (2020). **C** and **D:** Two other possible partitions of color space, with more complex classes of equivalence.

the classes of equivalence are planar: Irrespective of the surround, $x \parallel b$ is always perceived the same. In Fig. 3B, classes of equivalence are linear. The surround produces a repulsive effect, which becomes larger as the distance between the surround and the stimulus increases. In panels C and D, the effect of the surround is more complex.

We now assume that in all equivalence classes, a unique *uniform representative* exists, that is, a pair of the form $x \parallel x$, in which the stimulus coincides with its surround. In Fig. 3, uniform representatives lie along the white diagonal line, so the assumption means that all classes intersect the diagonal line. The hypothesis is supported by the empirical observation that subjects find feasible the task of matching a uniform stimulus $x \parallel x$ of controlled chromaticity with

a target stimulus x' presented against a surround of different chromaticity b' . In our lab, this feasibility has been verified for the set of target stimuli that can be produced by our computer screen. Although this set does not include maximally saturated colors, it is broad enough to encompass a rich collection of chromaticities. The uniform representative of each class must be unique, since all the members of a class are perceptually indistinguishable, and two uniform representatives of different chromaticity are (by definition of “different”) distinguishable. We define the function $\Phi_b(x)$ as the one that maps each member $x \parallel b$ of a given class to its uniform representative $x^0 \parallel x^0$, such that

$$x^0 = \Phi_b(x), \quad \Leftrightarrow \quad x \parallel b \sim x^0 \parallel x^0. \quad (11)$$

If, when shown on a fixed surround b , the stimuli x^α and x^β are perceived as different, then they necessarily belong to different classes, and Φ_b maps them to different uniform representatives. Therefore, for fixed b , the function $\Phi_b(x)$ must be injective. Since $x \parallel b$ and $x^0 \parallel x^0$ belong to the same class, the functions Φ_b and $\Phi_{b_\alpha \rightarrow b_\beta}$ must obey the relation

$$\Phi_{b_\alpha \rightarrow b_\beta} = \Phi_{b_\beta}^{-1} \circ \Phi_{b_\alpha}, \quad (12)$$

where the symbol \circ represents function composition, so that $\Phi_{b_\beta}^{-1} \circ \Phi_{b_\alpha}(x_\alpha) \equiv \Phi_{b_\beta}^{-1}[\Phi_{b_\alpha}(x_\alpha)]$. The injectivity of Φ_b guarantees that the inverse Φ_b^{-1} exists.

Uniform representatives remain unchanged by Φ , that is, $\Phi_x(x) = x$, for all x . The uniqueness of uniform representatives implies that all the points along the diagonal correspond to different classes, and that classes must cross the diagonal once and only once.

3.2 A notion of distance in color space

It then follows that any notion of distance between colors must be expressible as a notion of distance between classes of equivalence. In this paper, we start by defining a distance $d(x^\alpha \parallel x^\alpha, x^\beta \parallel x^\beta)$ between uniform representatives, that is, along the white diagonal in Fig. 3. To simplify the notation, from now on, whenever the distance function is evaluated on a pair of colors $d(x^\alpha, x^\beta)$ - as opposed to a pair of pairs $d(x^\alpha \parallel b^\alpha, x^\beta \parallel b^\beta)$ - we assume that both colors are uniform representatives, that is,

$$d(x^\alpha, x^\beta) := d(x^\alpha \parallel x^\alpha, x^\beta \parallel x^\beta). \quad (13)$$

The distance between non-uniform stimuli is then inherited from the distance between the corresponding representatives,

$$\begin{aligned} d(\mathbf{x}^\alpha \parallel \mathbf{b}^\alpha, \mathbf{x}^\beta \parallel \mathbf{b}^\beta) &= d[\Phi_{\mathbf{b}^\alpha}(\mathbf{x}^\alpha) \parallel \Phi_{\mathbf{b}^\alpha}(\mathbf{x}^\alpha), \Phi_{\mathbf{b}^\beta}(\mathbf{x}^\beta) \parallel \Phi_{\mathbf{b}^\beta}(\mathbf{x}^\beta)] \\ &= d[\Phi_{\mathbf{b}^\alpha}(\mathbf{x}^\alpha), \Phi_{\mathbf{b}^\beta}(\mathbf{x}^\beta)]. \end{aligned} \quad (14)$$

In other words, in order to calculate the distance between two pairs that do not both lie along the diagonal, we must first slide them through their respective classes of equivalence until they both hit the diagonal (in general, on different places), and then use the definition of distance for uniform representatives.

From the formal point of view, distances can only be defined between classes of equivalence, that is, between elements of the quotient space. Since there is a unique uniform representative per class, the distance is also well defined in the set of uniform representatives. However, the extension to pairs discussed above defines a pseudo-distance, since two different pairs can have zero distance. For simplicity, here we do not make explicit distinction between distances and pseudo-distance, hoping that the context will always make clear which concept is used in each case.

Distances between uniform representatives are defined in terms of just noticeable differences. That is, we define two uniform representatives to be at distance 1 when they are first discriminable with a pre-set accuracy. Pairs that are even closer do not reach the desired discriminability threshold. Each observer has their own individually tailored notion of distance, which we reveal with *Experiment I*. The obtained notion of distance can be used to define a perceptually uniform system of coordinates, as explained in Sect. 2.6. We thereby obtain a set of coordinates (here called the “natural coordinates”) in which the perceptual distance between uniform representatives is Euclidean. In these coordinates, classes of equivalence cross the diagonal of Fig. 3 at equi-distant points. In *Experiment II*, we repeat the discrimination experiments, but now with a surround of different chromaticity. The compared stimuli, hence, are no longer uniform representatives. We report the thresholds thus obtained in the natural coordinates, and, since the percept of each nonuniform $\mathbf{x} \parallel \mathbf{b}$ is equivalent to that of some uniform $\mathbf{x}^0 \parallel \mathbf{x}^0$, the comparison between the two experiments allows us to characterize the function $\Phi_{\mathbf{b}}(\mathbf{x})$. In *Experiment II*, surrounds are fairly close to stimuli, so the characterization can be regarded as restricted to pairs that are close to the diagonal. Therefore, *Experiment II* allows us to characterize the first order Taylor expansion of $\Phi_{\mathbf{b}}(\mathbf{x})$ around $\mathbf{x} = \mathbf{b}$. We study the adequacy of the natural coordinates to describe the experimental results, as well as the subject-to-subject variability. Finally, in order to test and expand these results, in *Experiment III*

we measure the perceptual shift produced by different surrounds that are further away from the diagonal, and report this shift in the natural coordinates. The obtained matches are consistent with the first-order expansion of the function $\Phi_b(\mathbf{x})$ found earlier, and allows us to extend the description to more dissimilar surrounds. More importantly, the experimental data confirm the assumption that, in the natural coordinates, the perceptual shift is homogeneous in color space, and isotropic among cardinal axes.

In order to be able to construct a geometry that captures the perceptual properties of stimuli and surrounds, we assume that the notion of distance complies with the following premises:

1. *The manifold of percepts is Riemannian*, so that the distance function d can be written in terms of a metric tensor J . This assumption was first introduced by von Helmholtz (1892) and Schrödinger (1920), later discussed by Silberstein (1943), Stiles (1946), and Resnikoff (1974), and is supported by the fact that discrimination thresholds conform an ellipse around the reference color (MacAdam, 1944; Krauskopf and Gegenfurtner, 1992), so local distances can be approximated by a quadratic form.
2. *The metric tensor is separable* in the isoluminant coordinates $x_1 = S$ and $x_2 = L - M$, implying that the differential distance can be written as

$$d\ell^2 = J_{11}(x_1) dx_1^2 + J_{22}(x_2) dx_2^2, \quad (15)$$

as shown by Krauskopf and Gegenfurtner (1992). This fact ensures that a coordinate system exists (the *natural coordinates*) in which the distance between uniform representatives is Euclidean (Sect. 2.6).

3. *The space of percepts is complete*, such that for any pair of points $\mathbf{x}^\alpha, \mathbf{x}^\beta$, a geodesic $\gamma_{\mathbf{x}^\alpha \rightarrow \mathbf{x}^\beta}$ joining them exists such that $d(\mathbf{x}^\alpha, \mathbf{x}^\beta) = \text{length}(\gamma_{\mathbf{x}^\alpha \rightarrow \mathbf{x}^\beta})$. In particular, the separability of the isoluminant plane implies that the lines defined by the cardinal axes \mathbf{e}^1 and \mathbf{e}^2 are geodesics.

One of the central hypotheses of this paper is that, in the natural coordinates (defined by the results of *Experiment I*) the effect of the surround has spherical symmetry. More precisely, the function $\Phi_b(\mathbf{x})$ is assumed to comply with two other requirements:

4. *The radial hypothesis*: If $\mathbf{x}^\alpha \parallel \mathbf{b}^\alpha \sim \mathbf{x}^\beta \parallel \mathbf{b}^\beta$, and $\mathbf{x}^\alpha, \mathbf{b}^\alpha$ and \mathbf{b}^β lie all on the same cardinal axis (either $\hat{\mathbf{e}}^1$ or $\hat{\mathbf{e}}^2$), the matched color \mathbf{x}^β also lies on the same axis. Evidence

for this symmetry is discussed in *Experiment III*. The hypothesis implies that a gray patch on a red surround acquires a greenish taint, whereas the same gray patch on a green surround looks reddish. Yet, none of these two surrounds (nor any other surround along the \hat{e}^2 dimension) can induce a bluish or a yellowish component on the gray patch. The analogous behavior is observed along the \hat{e}^1 dimension: blueish or yellowish surrounds cannot induce a reddish or a greenish taint on a stimulus. These results suggest that the displacement produced by $\Phi_b(x)$ acts along the line connecting the stimulus and the surround. That is, for fixed b , the vector field of displacements induced by $\Phi_b(x)$ is radial and centered in b . Therefore, in the vector fields of Fig. 4, arrows are parallel to the line joining b and x . In Riemannian geometries, the line connecting two points is generalized to a geodesic (Fig. 4A), so the precise formulation of the radial hypothesis reads: For fixed b and viewed as a function of x , the uniform representative $\Phi_b(x)$ lies along the geodesic $\gamma_{b \rightarrow x}$ that starts from b and passes through x . Moreover, if t is an arc-length affine parameter for $\gamma_{b \rightarrow x}(t)$, a scalar function $t(x, b)$ exists, such that the uniform representative can be written as $\Phi_b(x) = \gamma_{b \rightarrow x}[t(x, b)]$.

5. *Isotropy and homogeneity*: Color space is assumed to contain no privileged stimuli or directions, at least, when dealing with points that are far from the borders, the latter defined by stimuli that are maximally saturated. Evidence for this hypothesis is provided by *Experiments II* and *III* below. The core assumption is that the perceptual shift produced by a surround b on a stimulus s only depends on the distance $d(b, x)$, that is, $t(x, b) = t[d(x, b)]$. The natural coordinates are defined so as to ensure that equi-distant classes cross the diagonal in equi-distant points. Yet, from the definition of natural coordinates alone, there is no restriction on the shape of classes. The isotropy and homogeneity hypothesis implies that, when viewed in the natural coordinates, all the classes have the same shape, and only differ from one another in a rigid translation, as in all the examples of Fig. 3.

In the natural coordinates, the metric tensor reduces to the unit matrix, so all geodesics become straight lines, along which components can be summed and multiplied. In particular, the separability of the metric tensor (hypothesis 2) implies that the lines along the cardinal axes \hat{e}^1 and \hat{e}^2 are geodesics. In the natural coordinates, the mapping $\Phi_b(x)$ can be written as

$$\Phi_b(x) = \gamma_{b \rightarrow x}\{t[d(x, b)]\} = b + t[d(b, x)] \hat{u}, \quad \text{with } \hat{u} = \frac{x - b}{d(b, x)}. \quad (16)$$

That is, in the natural coordinates the perceptual shift induced by the surround is radial, it is centered at the surround b , and travels a distance $t[d(x, b)]$ along the direction \hat{u} that connects

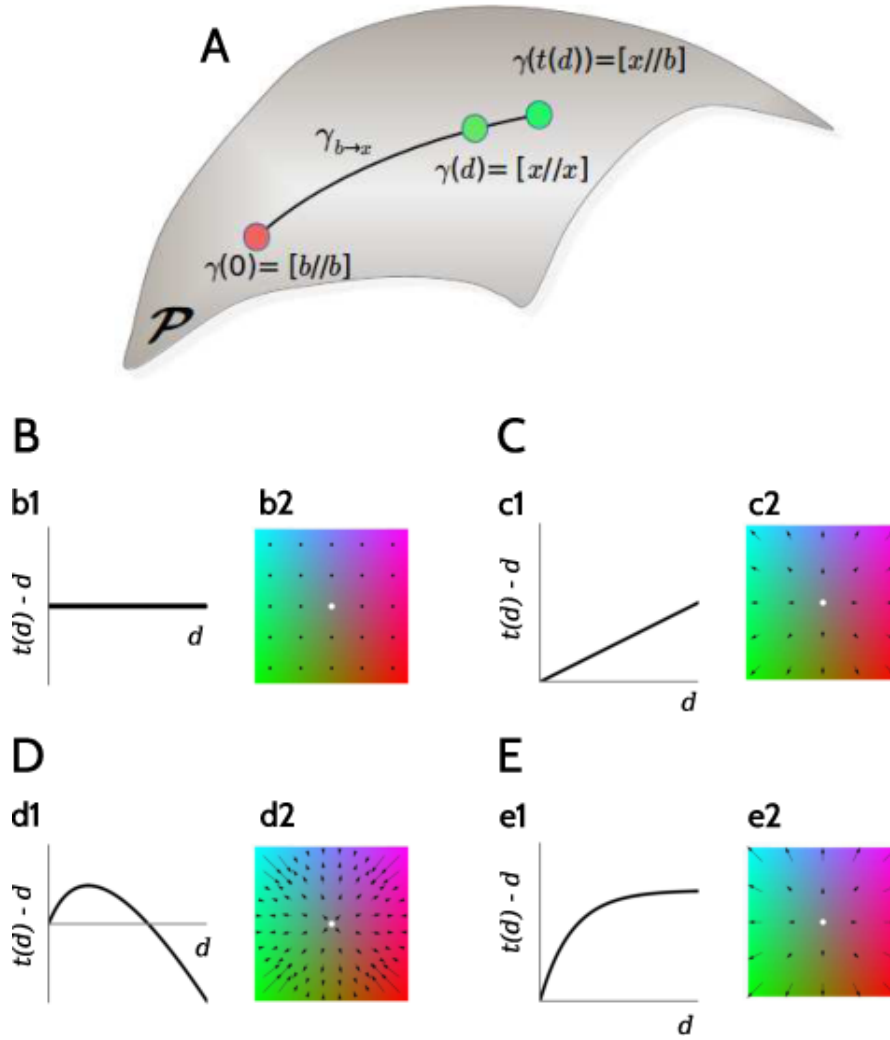


Figure 4: **Radially symmetric induction.** A: Hypothesis 4 and 5 state that when color x is surrounded by color b , the perceived sensation is chromatically equal to that of a uniform representative that lies along the geodesic $\gamma_{b \rightarrow x}$, displaced from x in an amount $t(d) - d$. The space \mathcal{P} contains all uniform representatives. In this example, the surround exerts a repulsive effect, since the $\gamma_{b \rightarrow x}[t(d)]$ is longer than $\gamma_{b \rightarrow x}(d)$. B-E: Four different examples of the shifts $t(d) - d$, corresponding to the classes of equivalence of Fig. 3. B: $t(d) = d$ (b1), and the vector field centered at the surround (white disk) vanishes in all the points of color space (b2). C: $t(d) \propto d$, with a proportionality factor different from unity. The vector field is linear. For $x = b$ the surround does not alter the perceived stimulus, but otherwise, the effect is radial, repulsive, and proportional to the distance between x and b . D: $t(d) \propto \ln(1 + d/\lambda)$, for some characteristic distance λ . The effect of the surround is initially repulsive, vanishes at $d = \lambda$, and then reverts to attractive. In E, $t(d) - d \propto [1 - \exp(-d/\lambda)]$, so the displacement is always repulsive, and tends to a constant value for large distances.

b and x . If the surround exerts no influence (Fig. 3A) then $\Phi_b(x) = x$, which necessarily implies that $t(d) = d$.

The effect of the surround is taken to be *repulsive* if $t(d) > d$ (the surround repels the stimuli, so that the uniform representative of a given stimulus is further away from the surround than the original stimulus), and *attractive* otherwise, that is, if $t(d) < d$.

3.3 Experiment I: Discrimination thresholds for $B = T$

Experiment I is used to find the natural coordinates of each observer, that is, the coordinates in which the discrimination thresholds around each color are constant and isotropic throughout color space. As explained in Sect.2.6, the derivation of the natural coordinates requires the knowledge of the metric tensor $J(\mathbf{x})$ of the submanifold of uniform representatives (Eqs. 6 and 7). We work with fixed luminosity, that is, $L + M = \text{const.}$ (Derrington et al., 1984). In order to estimate $J(\mathbf{x})$ in a 2-dimensional space, thresholds should be measured in at least 3 directions, so as to fit the 3 independent numbers that define the 2×2 quadratic form $E(\mathbf{x})$. Many more measurements are of course recommended, since trial-to-trial variations should be averaged out. In practice, only a few tens of measurements can be made before exhausting the volunteers, and getting non-stationary responses. As summarized by Hypothesis 2 above, Krauskopf and Gegenfurtner (1992) established that in the space $(x_1, x_2) = (S, L - M)$ defined by the cone contrasts, discrimination thresholds are described by diagonal quadratic forms. The ellipses, hence, are always elongated along the coordinate axes \hat{e}^1 and \hat{e}^2 . Moreover, their study also showed that the elongation of the ellipses along the \hat{e}^1 direction varied approximately linearly with x_1 , and bared no significant dependence on x_2 . The elongation along the \hat{e}^2 direction was shown to be approximately constant. These results can be used to greatly reduce the time required to measure the discrimination thresholds: It suffices to sample the thresholds around colors \mathbf{x} that lie along the cardinal axes, testing displaced colors $\mathbf{x} + \varepsilon_I \hat{e}$ that also lie along the same axis. The colors \mathbf{x} tested here are displayed in Fig. 1C.

We now deduce how the diagonal terms J_{ii} are obtained from the measured discrimination thresholds. For each uniform representative $\mathbf{x} \parallel \mathbf{x}$ sampled along the i -th coordinate axis ($i \in \{1, 2\}$), we determine the minimal displacement $\varepsilon_I(\mathbf{x}, \hat{e}^i)$ along the same direction \hat{e}^i , so that $\mathbf{x} + \varepsilon_I(\mathbf{x}, \hat{e}^i) \hat{e}^i \parallel \mathbf{x}$ be first distinguishable from $\mathbf{x} \parallel \mathbf{x}$. The sub-index “ I ” in ε_I indicates a threshold obtained with *Experiment I* (a different threshold is defined in *Experiment II*). Notice that in the uniform representative $\mathbf{x} \parallel \mathbf{x}$ the stimulus cannot be differentiated from the surround (Fig. 1A, left, right and upper patches), and the goal of the task is to determine the minimal value of $\varepsilon_I(\mathbf{x}, \hat{e}^i)$ required to detect the patch of chromaticity $\mathbf{x} + \varepsilon_I(\mathbf{x}, \hat{e}^i) \hat{e}^i$ against the surround \mathbf{x} (Fig. 1A, lower patch).

Defining the unit of distance in color space as that corresponding to the the first noticeable difference (Sect. 2.4), and making use of the assumption that distances derive from a diagonal metric tensor J ,

$$\begin{aligned}
1 &= d[\mathbf{x} \parallel \mathbf{x}, \mathbf{x} + \varepsilon_I(\mathbf{x}, \hat{\mathbf{e}}^i) \hat{\mathbf{e}}^i \parallel \mathbf{x}] \\
&= d\{\mathbf{x}, \Phi_{\mathbf{x}}[\mathbf{x} + \varepsilon_I(\mathbf{x}, \hat{\mathbf{e}}^i) \hat{\mathbf{e}}^i]\} \\
&= \text{Length of the geodesic } \gamma(t \{d[\mathbf{x}, \mathbf{x} + \varepsilon_I(\mathbf{x}, \hat{\mathbf{e}}^i) \hat{\mathbf{e}}^i]\}) \\
&= |t \{d[\mathbf{x}, \mathbf{x} + \varepsilon_I(\mathbf{x}, \hat{\mathbf{e}}^i)]\}| \\
&\approx |t'(0) \sqrt{J_{ii}(\mathbf{x})} \varepsilon_I(\mathbf{x}, \hat{\mathbf{e}}^i)|
\end{aligned}$$

Two factors determine the length $\varepsilon_I(\mathbf{x}, \hat{\mathbf{e}}^i)$ that needs to be traveled to reach the first noticeable difference: The metric J , and the derivative $t'(d)$. The metric defines how distances are quantified in each point of color space and along each direction, and appears in any Riemmanian space. The derivative is a special ingredient that appears in our case, due to the fact that we are comparing classes (or equivalently, uniform representatives) and not just stimuli. The derivative quantifies the displacement induced by the surround. If the surround exerts no influence (horizontal classes in Fig. 3A), then the derivative is equal to unity, since $\Phi_b(\mathbf{x}) = \mathbf{x}$ and $t(d) = d$. If the surround exerts a repulsive effect, the derivative is larger than unity. This case is illustrated in Fig. 3, where the contour lines have positive slope when crossing the diagonal. Repulsive surrounds facilitate discrimination, and therefore, increase the distance. Alternatively, to reach the same perceptual distance, a smaller threshold suffices. An attractive surround, instead, corresponds to $t'(d) < 1$.

Solving for J_{ii} ,

$$J_{ii}(\mathbf{x}) = \left[\frac{1}{t'(0) \varepsilon_I(\mathbf{x}, \hat{\mathbf{e}}^i)} \right]^2. \quad (17)$$

This equation allows us to find the diagonal terms J_{ii} of the metric tensor from the measured thresholds $\varepsilon_I(\mathbf{x}, \hat{\mathbf{e}}^i)$, up to a multiplicative factor $t'(0)$. Figures 5A and C show the measured thresholds. Along the x_1 axis, thresholds increased roughly linearly with x_1 , with some subject-to-subject variability. The largest thresholds were approximately 3 times larger than the smallest ones. Along the x_2 axis, thresholds showed a non monotonic behavior, with a minimum around $x_2 = 0$, which corresponds to the reference gray. Although there is a certain subject-to-subject variability, all observers show evidence of the minimum. For each fixed subject, the modulation of thresholds was significantly smaller than along the S axis, with the maximal and minimal threshold of each observer differing in less than 50% of the minimal threshold. Hence, confirming the result of Krauskopf and Gegenfurtner (1992), thresholds along the $\hat{\mathbf{e}}^1$ direction vary

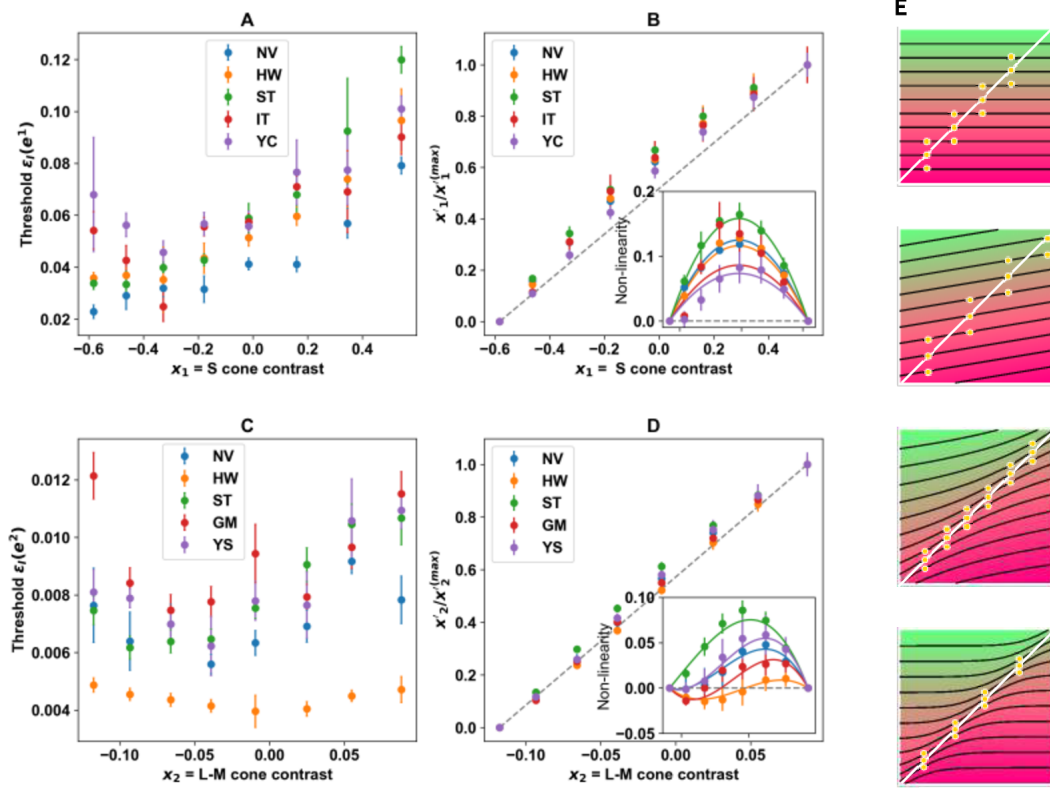


Figure 5: **Discrimination thresholds when the target and the surround chromaticities coincide.** A and C: Discrimination thresholds for the x_1 (A) and x_2 (C) cone contrast coordinates. Different observers displayed in different colors. B and D: Natural coordinates $x'_1/x'_{1\max}$ (B) and $x'_2/x'_{2\max}$ (D) as a function of the cone contrasts. The normalizing factors $x'_i/x'_{i\max}$ are the maximal natural coordinate obtained for each subject, and were used to scale the data in order to compare different observers, which would otherwise produce natural coordinates spanning intervals of different lengths. Insets: Deviations from the linear mapping. Each data point is obtained from the fit of Eq. 1, and error bars are the expected errors of the fit. Parameters of the optimal fits are given in Table 1. E: The measured thresholds represent the vertical displacement between a pair $x \parallel x$ on the diagonal (yellow dot), and another pair sitting right above, or just below, on a class of equivalence that is at perceptual distance 1 from that of $x \parallel x$.

more pronouncedly than along the \hat{e}^2 direction. Yet, our data reveal that they do not remain strictly constant along the \hat{e}^2 directions, since the mild non-monotonic behavior was found to be significant.

The threshold $\epsilon_I(x, \hat{e}^i)$ is the change in chromaticity required for a stimulus to be discriminated from its surround with a fixed precision (Sect. 2.4). In Fig. 5E, this increment is the vertical displacement between a pair $x \parallel x$ on the diagonal, and a point $x + \epsilon_I(x, \hat{e}^i)\hat{e}^i \parallel x$ sitting right above (or below) the former, on the equivalence class at distance 1 from that of $x \parallel x$. If Fig. 5E were depicted in the cone fundamentals, or in any other system of coordi-

nates that had not been chosen to reflect perceptual distances, different triplets of yellow dots along the diagonal would appear to span different vertical height, since the vertical separation between just-noticeably-different classes (classes at distance 1) can be arbitrary. Finding the natural coordinates is equivalent to finding a representational system in which the vertical span of all triplets remain constant along the diagonal. In these coordinates, the classes intersect the diagonal at equi-distant intervals, as in Figs. 3 and 5E.

To define the natural coordinates along the axes \hat{e}^1 and \hat{e}^2 , the square root of the diagonal elements of the metric have to be integrated (Eq. 5). To this aim, an analytic expression of $J^{1/2}(\mathbf{x})$ is needed. We therefore propose a polynomial function

$$|t'(0)| \sqrt{J_{ii}(x_i)} = \frac{1}{\varepsilon_I(\mathbf{x}, \hat{e}^i)} = \sum_{j=0}^n \alpha_j x_i^j, \quad (18)$$

the order n of which should be the smallest that can still account for the data with p -values above 0.01. Along the \hat{e}^1 axis, a straight line ($n = 1$) suffices, whereas the \hat{e}^2 axis requires to go up to a quadratic expression ($n = 2$). Table 1 of the Appendix contains the fitted parameters.

Along the \hat{e}^1 direction, the variability of the coefficients fitted for different observers provides evidence that the natural coordinates are individually tailored, since a single set of coefficients α_j cannot account for the metric tensor of different subjects. The p -value for the hypothesis that there is single α_0 valid for the 5 subjects is 10^{-8} , and for a single α_1 is $6 \cdot 10^{-3}$. Instead, along the \hat{e}^2 direction, the individual differences are significant in the constant (p -value below 10^{-10}) and linear coefficients (p -value $2 \cdot 10^{-7}$), but not in the quadratic ones (p -value = 0.68).

Once an analytic expression has been obtained for the diagonal elements of the metric, the natural coordinates along the cardinal axes can be calculated by integration (Eqs. 6 and 7), except for the yet unknown factor $|t'(0)|$. In Figs. 5B and D, the normalized natural coordinates x'_1 and x'_2 are shown as a function of the corresponding cone contrasts x_1 and x_2 . The insets display the deviation from a linear mapping, together with the quadratic or cubic analytical expressions obtained by integrating Eq. 18 (same parameters as in Table 1). Importantly for what follows, in the natural coordinates, the distance between two colors \mathbf{x}' and \mathbf{y}' is calculated with the Euclidean formula. If the two colors lie along the cardinal axis \hat{e}^i , then $d(\mathbf{x}'\hat{e}^i, \mathbf{y}'\hat{e}^i) = |x'_i - y'_i|$.

3.4 Experiment II: Discrimination Thresholds for $B \neq T$

Experiment I involved a comparison between two stimuli, both surrounded by the same color. One stimulus coincided with the surround, and the other differed in only the minimal amount that rendered it visible. *Experiment II* involves exactly the same discrimination task, but now with a surround \mathbf{b} that is different from the two tested stimuli, and is varied systematically. Since now the discrimination threshold depends on the surround, we use the notation $\varepsilon_{II}(\mathbf{x}, \mathbf{b}, \hat{\mathbf{e}}^i)$. *Experiment II* reduces to *Experiment I* when $\mathbf{b} = \mathbf{x}$, that is, $\varepsilon_{II}(\mathbf{x}, \mathbf{x}, \hat{\mathbf{e}}^i) \equiv \varepsilon_I(\mathbf{x}, \hat{\mathbf{e}}^i)$. In *Experiment II*,

$$\begin{aligned} 1 &= d[\mathbf{x} \parallel \mathbf{b}, \mathbf{x} + \varepsilon_{II}(\mathbf{x}, \mathbf{b}, \hat{\mathbf{e}}^i) \hat{\mathbf{e}}^i \parallel \mathbf{b}] \\ &= d\{\Phi_{\mathbf{b}}(\mathbf{x}), \Phi_{\mathbf{b}}[\mathbf{x} + \varepsilon_{II}(\mathbf{x}, \mathbf{b}, \hat{\mathbf{e}}^i) \hat{\mathbf{e}}^i]\}, \end{aligned} \quad (19)$$

where the second line derives from the hypothesis that distances between two pairs remain invariant if any of the pairs is replaced by another member of its own class, in particular, the uniform representative. Since \mathbf{b} , \mathbf{x} and $\mathbf{x} + \varepsilon_{II}(\mathbf{x}, \mathbf{b}, \hat{\mathbf{e}}^i) \hat{\mathbf{e}}^i$ lie all three on the same cardinal axis,

$$d\{\Phi_{\mathbf{b}}(\mathbf{x}), \Phi_{\mathbf{b}}[\mathbf{x} + \varepsilon_{II}(\mathbf{x}, \mathbf{b}, \hat{\mathbf{e}}^i) \hat{\mathbf{e}}^i]\} = |d[\Phi_{\mathbf{b}}(\mathbf{x} + \varepsilon_{II}(\mathbf{x}, \mathbf{b}, \hat{\mathbf{e}}^i) \hat{\mathbf{e}}^i, \mathbf{b}) - d[\Phi_{\mathbf{b}}(\mathbf{x}), \mathbf{b}]|.$$

Replacing this result in Eq. 19,

$$\begin{aligned} 1 &= |t\{d[\mathbf{x} + \varepsilon_{II}(\mathbf{x}, \mathbf{b}, \hat{\mathbf{e}}^i) \hat{\mathbf{e}}^i, \mathbf{b}]\} - t[d(\mathbf{x}, \mathbf{b})]| \\ &\approx |t'[d(\mathbf{x}, \mathbf{b})] \sqrt{J_{ii}(\mathbf{x})} \varepsilon_{II}(\mathbf{x}, \mathbf{b}, \hat{\mathbf{e}}^i)| \end{aligned} \quad (20)$$

Since J_{ii} is known from Experiment I, we can use Eq. 17 to get

$$\varepsilon_{II}(\mathbf{x}, \mathbf{b}, \hat{\mathbf{e}}^i) = \varepsilon_I(\mathbf{x}, \hat{\mathbf{e}}^i) \left| \frac{t'(0)}{t'[d(\mathbf{x}, \mathbf{b})]} \right|. \quad (21)$$

Notice that, as $t(d)$ is an arc length, the derivative $t'(d)$ is an invariant quantity - that is, independent of the coordinates. Therefore, although each threshold varies with the choice of coordinates, their ratio does not.

When the surround coincides with the stimulus, we get $\varepsilon_I = \varepsilon_{II}$. As the surround \mathbf{b} is moved away from the stimulus \mathbf{x} , the distance $d(\mathbf{x}, \mathbf{b})$ increases. The threshold ε_{II} may then either increase or decrease from ε_I , depending on whether the absolute value of the slope of $t(d)$ is larger or smaller than that of $t(0)$. Therefore, by measuring the thresholds ε_{II} for different surrounds, the derivative of $t(d)$ is revealed. Yet, this reasoning is only valid if the *isotropy and homogeneity hypothesis* proposed above (number 5 in Sect. 3.2) indeed holds, namely,

the assumption that the perceptual shift induced by the surround only depends on the distance $d(\mathbf{x}, \mathbf{b})$. Therefore, before characterizing the shape of $t(d)$, we first use *Experiment II* to assess the validity of this hypothesis. To do so, we demonstrate that, in the natural coordinates, the dependence of the thresholds $\varepsilon_{II}(\mathbf{x}, \mathbf{b}, \hat{\mathbf{e}}^i)$ with \mathbf{b} and with \mathbf{x} can be entirely written in terms of the difference $x_i - b_i$.

The first step is to describe the dependence of the thresholds on the surround in the cone contrast coordinates. In Fig. 6, we see the variation of the thresholds from those obtained in *Experiment I* of a given subject as a function of the difference $x_i - b_i$. As reported previously (Krauskopf and Gegenfurtner, 1992), the thresholds are minimal for $\mathbf{b} = \mathbf{x}$, and increase as the surround differs from the stimulus. This non-monotonic behavior discards the possibility that classes be linear functions of the stimulus, as proposed by Resnikoff (1974). It then becomes important to characterize the variation. A naked eye examination, however, does not suffice to determine whether thresholds increase linearly or quadratically from the uniform condition. In *Experiment II*, the surround is always relatively close to the stimulus, so an expansion of $\varepsilon_{II}(\mathbf{x}, \mathbf{b}, \hat{\mathbf{e}}^i)$ around $\mathbf{b} = \mathbf{x}$ is sufficient to explain the measured thresholds, and to compare the linear with the quadratic hypotheses. To that end, we consider two possible expansions, namely

$$\text{Model 1 : } \varepsilon_{II}(\mathbf{x}, \mathbf{b}, \hat{\mathbf{e}}^i) - \varepsilon_I(\mathbf{b}, \hat{\mathbf{e}}^i) \approx \gamma_0 + \gamma_1(x_i - b_i) + \gamma_2(x_i - b_i)^2 \quad (22)$$

$$\text{Model 2 : } \varepsilon_{II}(\mathbf{x}, \mathbf{b}, \hat{\mathbf{e}}^i) - \varepsilon_I(\mathbf{b}, \hat{\mathbf{e}}^i) \approx \gamma_0 + \gamma_1(x_i - b_i) + \gamma_2|x_i - b_i| \quad (23)$$

Both models contain 3 fitting parameters. The first model assumes that $\varepsilon_{II}(\mathbf{x}, \mathbf{b}, \hat{\mathbf{e}}^i)$ has a continuous derivative at $b_i = x_i$, and is able to describe the quadratic departure from linearity. The second model allows for the possibility of a discontinuous derivative, and for the ascending and the descending linear portions to have different slopes. It cannot, however, describe quadratic effects. In Fig. 6, we compare the performance of the two proposals in fitting the measured thresholds.

The fitted coefficients γ_0 , γ_1 and γ_2 are reported in Tables 2 and 3 of the Appendix. The constant term γ_0 is of the order of the experimental error of the measurements, implying that when the stimulus and the surround coincide, ε_{II} indeed reduces to ε_I .

Each fit (that is, each subject, tested along each axis) produces a χ^2 value quantifying the goodness of the fit, and although there are small differences among conditions, the mean χ^2 -value obtained for Model 2 (averaged across subjects and axes) is half the value obtained for Model 1. Accordingly, the mean p -value obtained for the hypothesis that the data be generated with Model 2 is twice as large as with Model 1. These results imply that the data is better

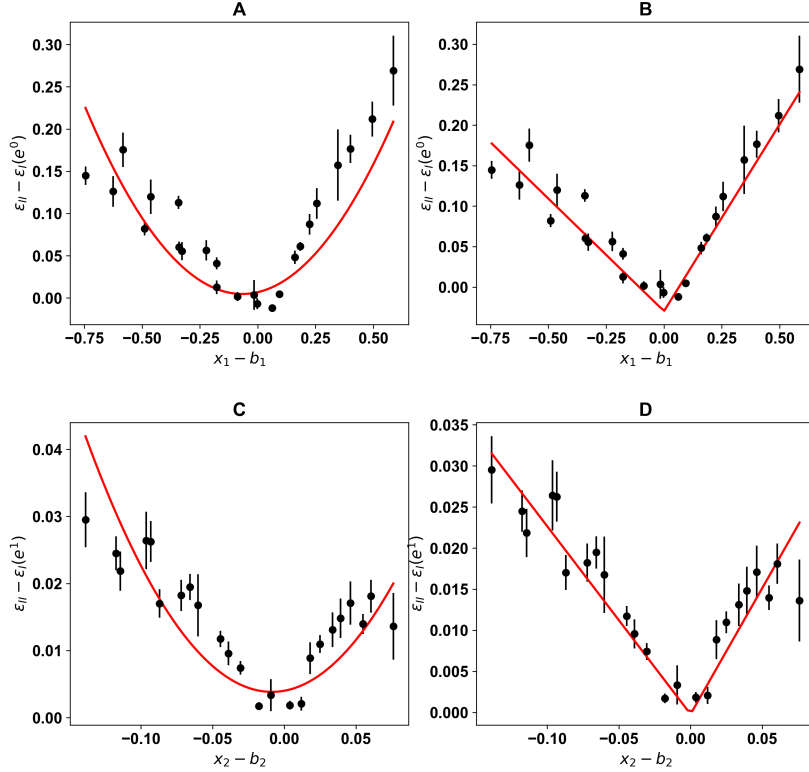


Figure 6: **Performance of models 1 and 2 in describing measured thresholds $\varepsilon_{II}(x, b, \hat{e}^i)$.** Thresholds were measured for observer HW, and are shown as a function of $x_i - b_i$. Data points are obtained from the fit of Eq. 1, and error bars are the expected error of the fit. Red line: fitted model. A and C: Model 1 (Eq. 22). B and D: Model 2 (Eq. 23). A and B: Discrimination thresholds measured along \hat{e}^1 . C and D: Along \hat{e}^2 .

explained by Model 2, and a discontinuous derivative is to be expected at $\mathbf{b} = \mathbf{x}$. Moreover, the fact that γ_1 is typically significantly different from zero indicates that the ascending and the descending linear portions of Model 2 have different slopes.

To determine whether the hypothesis of homogeneity and isotropy is justified, we now transform \mathbf{x} , \mathbf{b} and ε_{II} to the natural coordinates, using Eqs. 6 and 7 and the metric tensor J_{ii} obtained with *Experiment I*. We emphasize that no data of *Experiment II* is used to fit the parameters of the transformation. Although we still lack the multiplicative constant $|t'(0)|$, we can nevertheless assess whether, in these coordinates, $\varepsilon'_{II}(\mathbf{x}', \mathbf{b}', \hat{e}^i)$ indeed depends only on the difference $|x'_i - b'_i|$. If it does, the transformation should suffice to eliminate the asymmetry in the slopes of the descending and ascending portions of Model 2. Equivalently, when ε'_{II} (measured for a single subject with different stimuli \mathbf{x} , surrounds \mathbf{b} and axes \hat{e}^i) is plotted as a function of $|x'_i - b'_i|$, a single straight line should be seen. This plot is displayed in the first column of Fig. 7, for surrounds varying along the axis \hat{e}^1 (top), \hat{e}^2 (middle) and both axes together (bottom).

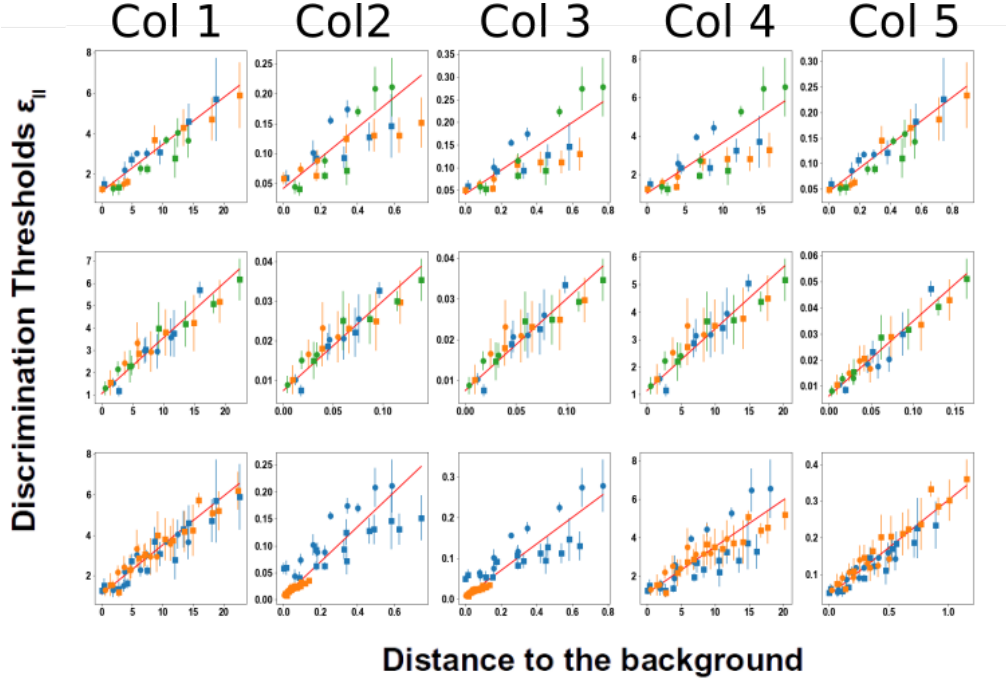


Figure 7: **Assessment of the validity of hypothesis 5.** Thresholds measured in *Experiment II* for subject NV as a function of the distance between the surround and the stimulus. Circles: $b_i > x_i$. Squares: $b_i < x_i$. Each column represents a different choice of the system of coordinates in which thresholds, stimuli and surround are represented. Column 1: natural coordinates defined with the data of Experiment I. Columns 2, 3, 4: Other coordinates employed in the literature (see text), requiring no fitted parameters. Column 5: Optimal coordinate system defined with a single fitted parameter. Top row: \mathbf{b} and \mathbf{x} lie along axis \hat{e}^1 . Green: $\mathbf{b} = (x_1, x_2) = (0.16, 0)$, blue: $\mathbf{b} = (0, 0)$, orange: $\mathbf{b} = (-0.24, 0)$. Middle row: axis \hat{e}^2 . Green: $\mathbf{b} = (0, 0)$, blue: $\mathbf{b} = (0, -0.015)$, orange: $\mathbf{b} = (0, 0.015)$. Bottom: both axes together. Blue data points: \hat{e}^1 . Orange: \hat{e}^2 .

For comparison, we also show the same data points represented in other coordinate systems, to test whether the linear relation between $\varepsilon'_{II}(\mathbf{x}', \mathbf{b}', \hat{e}^i)$ with $|x'_i - b'_i|$ indeed becomes more evident in the natural coordinates than in other coordinate systems. In column 2, the horizontal axis contains the difference $|x_i - b_i|$ in the cone contrast coordinates used by Krauskopf and Gegenfurtner (1992), and the vertical axis, the thresholds ε_{II} also in the cone contrast coordinates. Clearly, the data points obtained for $b_i > x_i$ (circles) define a different slope from that for $b_i < x_i$ (squares). Moreover, the slopes obtained in the axes \hat{e}^1 and \hat{e}^2 are markedly different (bottom row), and so are the total ranges of the data. As a consequence, the amount of dispersion is significantly larger in the panels of column 2 than in column 1. Accordingly, the χ^2 obtained from linear fits in column 2 are more than three times larger than those in column 1, meaning that the *Homogeneity and isotropy hypothesis* becomes significantly more evident in the natural coordinates than in the cone contrasts.

In the cone contrast coordinate system, the origin $\mathbf{x} = \mathbf{0}$ is gray. Since there is no reason why gray should occupy a central role, columns 3 and 4 evaluate the performance of two additional coordinate systems, in which the role of the reference gray of cone contrast coordinates $(\bar{S}_g, \bar{M}_g, \bar{L}_g)$ is now replaced by the surround, be it its chromaticity (3rd column) or its threshold (4th column). More specifically, if the supra-index *cc* represents cone contrasts, in column 3, the coordinates of both the stimulus and the surround are defined by the relation $x_i^{\text{new}} = x_i^{\text{cc}} / (b_i^{\text{cc}} + 1)$, so that changes in stimuli are represented by the relative contrast to the background in which the discrimination task was performed. If ε_{II} depended only on the ratio x_i / b_i , we would conclude that Webber’s law (Wyszecki and Stiles, 2000) would be verified. In column 4, the transformation is $x_i^{\text{new}} = x_i^{\text{cc}} / \varepsilon_I(\mathbf{b}, \hat{\mathbf{e}}^i)^{\text{cc}}$, so that the threshold of the surround always corresponds to unity. If ε_{II} depended only on the ratio $\varepsilon_I(\mathbf{x}, \hat{\mathbf{e}}^i) / \varepsilon_I(\mathbf{b}, \hat{\mathbf{e}}^i)$, a modified version of Webber’s law, formulated in terms of thresholds, would be governing discriminability. The resulting average χ^2 values represent a three-fold (column 3) and a two-fold (column 4) increase with respect to the first column. Again, the natural coordinates describe better the linear relation.

While the first four columns assess the success of coordinate systems that contained no free parameters, the last column was constructed by searching for the value of a free coefficient α , fitted from the data, that produced the mapping $x_i^{\text{new}} = x_i^{\text{cc}} + \frac{\alpha}{2}(x_i^{\text{cc}})^2$ with minimal χ^2 -value. The improvement, however, was only marginal, since the χ^2 -value of the 5th column is only 6% smaller than that of the first column. The natural coordinates, hence, are almost as optimal as the ones of the last column, and they contain no parameters fitted with the data of *Experiment II*.

By adding additional yellow dots to Fig. 5E, the vertical triplets can be extended to vertical sequences, unfolding both upwards and downwards, marking consecutive classes that always lie at perceptual distance 1 from their neighbors. The thresholds $\varepsilon_{II}(\mathbf{x}, \mathbf{b}, \hat{\mathbf{e}}^i)$ represent the vertical separation of consecutive dots. Linearly growing thresholds imply that classes become increasingly separated as we depart from the diagonal. Yet, in *Experiment II*, the limited range of colors produced by computer monitors imply that the surround is never far away from the stimulus. The linear trend, hence, cannot be ensured throughout the entire space: It refers to short sequences of yellow dots located around the diagonal, where ε_{II} is well approximated by a linear function of its arguments. When defining the natural coordinates, we guaranteed that classes were equi-distant right on the diagonal. Yet, beyond the diagonal, in principle they could still be arbitrary. *Experiment II* shows that the separation $\varepsilon_{II}(\mathbf{x}, \mathbf{b}, \hat{\mathbf{e}}^i)$ between consecutive dots depends only on the distance $|x'_i - b'_i|$. If the distance $|x'_i - b'_i|$ is changed in a fixed amount, the

separation between the dots is always the same, irrespective of the individual values of x'_i and b'_i . In other words, at least in some region around the diagonal, the lines representing the classes are parallel. In this region, *Experiment II* supports the isotropy and homogeneity hypothesis.

The linear dependency of $\varepsilon_{II}(d)$ with d found in *Experiment II* restricts the set of feasible functions $t(d)$. For example, in the two upper panels of Fig. 5E, the separation between consecutive lines is constant, so the results of *Experiment II* discard these two options. The two lower panels correspond to cases in which $\varepsilon_{II}(d) \propto d$, for small d . Therefore, thus far, they both constitute possible candidate descriptions of the effect of the surround on the classes of equivalence. We now compare these options.

Let us first assume that the initial linear trend of Fig. 7 continues also for larger distances. This hypothesis implies that ε_{II} is proportional to $1 + \lambda d(\mathbf{x}, \mathbf{b})$. It then follows that $t'(d)/t'(0) = (1 - \lambda d)^{-1}$, which in turn yields $t(d) = t'(0) \ln(1 + \lambda d)$. The resulting displacement $t(d) - d$ is illustrated in panel *d1* of Fig. 4. The effect of the surround is initially repulsive, becomes neutral at an intermediate distance in which $t(d) = d$, and reverts to attractive for even larger distances (see the inversion of the arrows representing the vector field in panel *c2* of Fig. 3). Actually, $t(d)$ can even become negative. This behavior challenges our intuition in several ways, namely:

- Thresholds grow unbounded, implying that sufficiently distant surrounds preclude the discrimination of stimuli altogether, no matter how different.
- The displacement induced by the surround grows indefinitely for large distances. Therefore, the perceived color may differ from the presented one in an arbitrary amount, by simply displacing the surround far enough.
- The effect inverts its polarity (from repulsive to attractive) as the distance grows. The distance where the inversion takes place is singled out.
- Two different surrounds (one on each side of the neutral point) acting on the same stimulus may induce the same apparent color, even though intermediate surrounds produce different apparent colors.
- If the distance between the stimulus and the surround is sufficiently large, $t(d)$ vanishes. At that point, the stimulus becomes equal to the surround, producing a spatially uniform percept. At even larger distances, the perceived stimulus is on the negative side of the geodesic. In other words, a green stimulus surrounded by red can give rise to a red percept that is even more saturated than the surround.

In order to avoid these bizarre effects, thresholds should deviate from the linear behavior at large distances, decelerating. The simplest deviation from the linear hypothesis would be for thresholds to saturate at a given value, after the initial linear growth. Such saturation can be modelled as $\varepsilon_{II}(d) \propto [1 + a \exp(-d/\lambda)]^{-1}$, as in panel *e1* of Fig. 4. The limited range in which *Experiment II* was performed (Fig. 7) does not show strong evidence of deviations. Yet, one can still test whether the thresholds of Fig. 7 can also be compatible with a sublinear trend. To this end, in Fig. 8 we compare the hypotheses that $t'(d) \propto (1 + d/\lambda)^{-1}$ (compatible with linear thresholds) and $t'(d) \propto 1 + ae^{-d/\lambda}$ (compatible with exponentially saturating thresholds). Slightly smaller χ^2 values are obtained for the exponential fit. Therefore, although *Experiment*

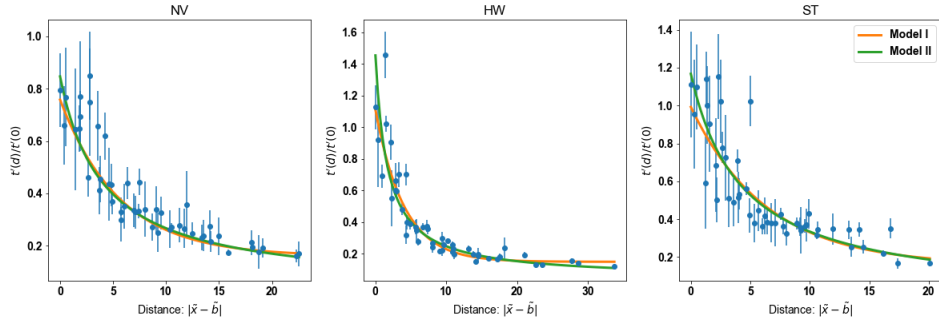


Figure 8: Comparison between the hypotheses $t(d) \propto (1 + \lambda d)^{-1}$, which is consistent with the linear hypothesis $\varepsilon_{II}(d) \propto 1 + \lambda d$, and $t'(d) \varepsilon_{II} \propto (1 + ae^{-d/\lambda})^{-1}$, for subjects NV (left), HW (middle) and ST (right).

II is not designed to test the hypothesis of saturating thresholds, the data are more compatible with the exponential model than with the linear one.

3.5 Experiment III: Asymmetric matching task

In the asymmetric matching task (Sect. 2.5), for each pair $\mathbf{x}^\alpha \parallel \mathbf{b}^\alpha$ and each surround \mathbf{b}^β the observer finds the stimulus \mathbf{x}^β that fulfills $\mathbf{x}^\alpha \parallel \mathbf{b}^\alpha \sim \mathbf{x}^\beta \parallel \mathbf{b}^\beta$. In other words, she or he reports $\mathbf{x}^\beta = \Phi_{\mathbf{b}^\alpha \rightarrow \mathbf{b}^\beta}(\mathbf{x}^\alpha)$. Equation 11 implies that this condition is equivalent to

$$\Phi_{\mathbf{b}^\beta}(\mathbf{x}^\beta) = \Phi_{\mathbf{b}^\alpha}(\mathbf{x}^\alpha). \quad (24)$$

If the stimulus and the surround are both on the same cardinal axis $\hat{\mathbf{e}}^i$, Eq. 16 yields

$$\Phi_{\mathbf{b}}(\mathbf{x})|_i = \gamma\{t[d(\mathbf{x}, \mathbf{b})]\}_i = b_i + t[d(\mathbf{x}, \mathbf{b})] \text{Sgn}[x_i - b_i]. \quad (25)$$

If this condition is inserted in Eq. 24,

$$b_i^\beta + t[d(\mathbf{x}^\beta, \mathbf{b}^\beta)] \text{Sgn}[x_i^\beta - b_i^\beta] = b_i^\alpha + t[d(\mathbf{x}^\alpha, \mathbf{b}^\alpha)] \text{Sgn}[x_i^\alpha - b_i^\alpha].$$

In the natural coordinates, $d(\mathbf{x}, \mathbf{b}) = |x_i - b_i|$. Using this equality, and a few algebraic manipulations,

$$\left| [t(d^\beta) - d^\beta] - [t(d^\alpha) - d^\alpha] \text{Sgn}[x_i^\alpha - b_i^\alpha] \text{Sgn}[x_i^\beta - b_i^\beta] \right| = |x_i^\alpha - x_i^\beta| \quad (26)$$

Therefore, the perceptual displacement $|x_i^\beta - x_i^\alpha|$ induced by the two surrounds only depends on the distances $d^\alpha = d(\mathbf{x}^\alpha, \mathbf{b}^\alpha)$ and $d^\beta = d(\mathbf{x}^\beta, \mathbf{b}^\beta)$ between each stimulus and its surround: As long as d^α and d^β remain constant, the displacements depend on none of the individual values $x_i^\alpha, x_i^\beta, b_i^\alpha$ or b_i^β , nor on the direction \hat{e}^i . As a consequence, if displacements are plotted as a function of d^α and d^β , the set of data points should define 2-dimensional manifold, no matter how many stimuli, surrounds and cardinal axes be included. Moreover, the 2-dimensional structure should only be evident in the natural coordinates, since in any other coordinate system, $d \neq |x_i - b_i|$, implying that Eq. 26 does not hold. In Fig. 9, the obtained graphs are displayed. Along each coordinate axes, the shifts define a 2-dimensional manifold, both in the cone con-

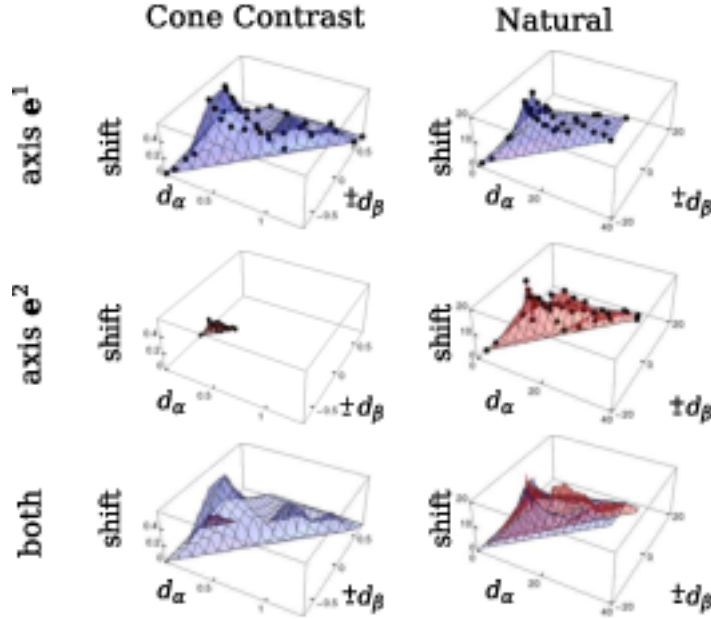


Figure 9: **Perceptual displacements induced by surrounds.** Shifts $|x_i^\alpha - x_i^\beta|$ as a function of the distances $d^\alpha = |x_i^\alpha - b_i^\alpha|$ and $\pm d^\beta = \pm |x_i^\beta - b_i^\beta|$, for observer ST, along the axis \hat{e}^1 (top), \hat{e}^2 (middle) and both together (bottom), in the cone contrast coordinates (left) and the natural ones (right). The factor ± 1 multiplying d^β is defined by the product of Sign functions in Eq. 26. The measured data points appear in the top and middle panels, and the surface interpolates the measured values. In the lower panels, the two sheets are shown to coalesce in the natural coordinates, but not in the cone contrast.

trast and the natural coordinates. If both axes are mixed, however, in the natural coordinates the collection of data points still lie on a 2-dimensional manifold, since the two sheets corresponding to the different axes coalesce. This is not the case in the cone contrast coordinates, since

the sheet corresponding to \hat{e}_2 is significantly closer to the origin than that of \hat{e}_1 . To quantify this difference, we estimated the dimension D of the manifold containing the data (Granata and Carnevale, 2016), obtaining $D = 2.11$ in the natural coordinates, and $D = 3.19$ in the cone contrast coordinates.

In order to test whether the exponential model suggested by Fig. 8 provided a good description of the results of *Experiment III*, for each human observer we simulated a computational agent performing the same forced choice task. The agent decided in each trial which of the two proposed colors was most similar to the target, and did so using the metric that the modeled subject revealed in *Experiment I*. This metric was used to represent the experiment in the natural coordinates. In these coordinates, the effect of the surround was modelled as $\Phi_b(\mathbf{x})|_i = x_i + \kappa \text{Sign}(x_i - b_i) [1 - \exp(-|x_i - b_i|/\lambda)]$. For each target color \mathbf{x}^α presented on a surround \mathbf{b}^α and two candidate colors \mathbf{x}^p and \mathbf{x}^q on the surround \mathbf{b}^β , the agent had to decide whether $d[\Phi_{\mathbf{b}^\alpha}(\mathbf{x}^\alpha), \Phi_{\mathbf{b}^\beta}(\mathbf{x}^p)]$ was larger or smaller than $d[\Phi_{\mathbf{b}^\alpha}(\mathbf{x}^\alpha), \Phi_{\mathbf{b}^\beta}(\mathbf{x}^q)]$. Guided by the choices of the agent, the iterative procedure of the experiment produced the final $\mathbf{x}^\beta = \Phi_{\mathbf{b}^\alpha \rightarrow \mathbf{b}^\beta}(\mathbf{x}^\alpha)$. Since significant amounts of trial-to-trial variability were observed in the responses of human subjects (Fig. 5), some additive Gaussian noise was included in the evaluation of the differences $d[\Phi_{\mathbf{b}^\alpha}(\mathbf{x}^\alpha), \Phi_{\mathbf{b}^\beta}(\mathbf{x}^p)] - d[\Phi_{\mathbf{b}^\alpha}(\mathbf{x}^\alpha), \Phi_{\mathbf{b}^\beta}(\mathbf{x}^q)]$. The functional form proposed for $t(d)$ contains two free parameters, κ and λ , and the output of the simulation fluctuates in every iteration because of the added noise. Hence, the fitting procedure was implemented with the python package *noisyopt* [Spall (1998), Mayer et al. (2016)], that optimizes noisy functions. A single exponential function was fitted for each observer, for the three different couples of surrounds on each axis, and for both axes. Figure 10 displays the resulting \mathbf{x}^β values as a function of the target \mathbf{x}^α for subject ST, on four different pairs of surrounds, two for each axis. The shift induced by the surround becomes significant in the interval of target \mathbf{x}^α values in which the push/pull produced by one of the surrounds is not compensated by the other, that is, where the green and orange lines differ. The simulations reproduce qualitatively the measured data.

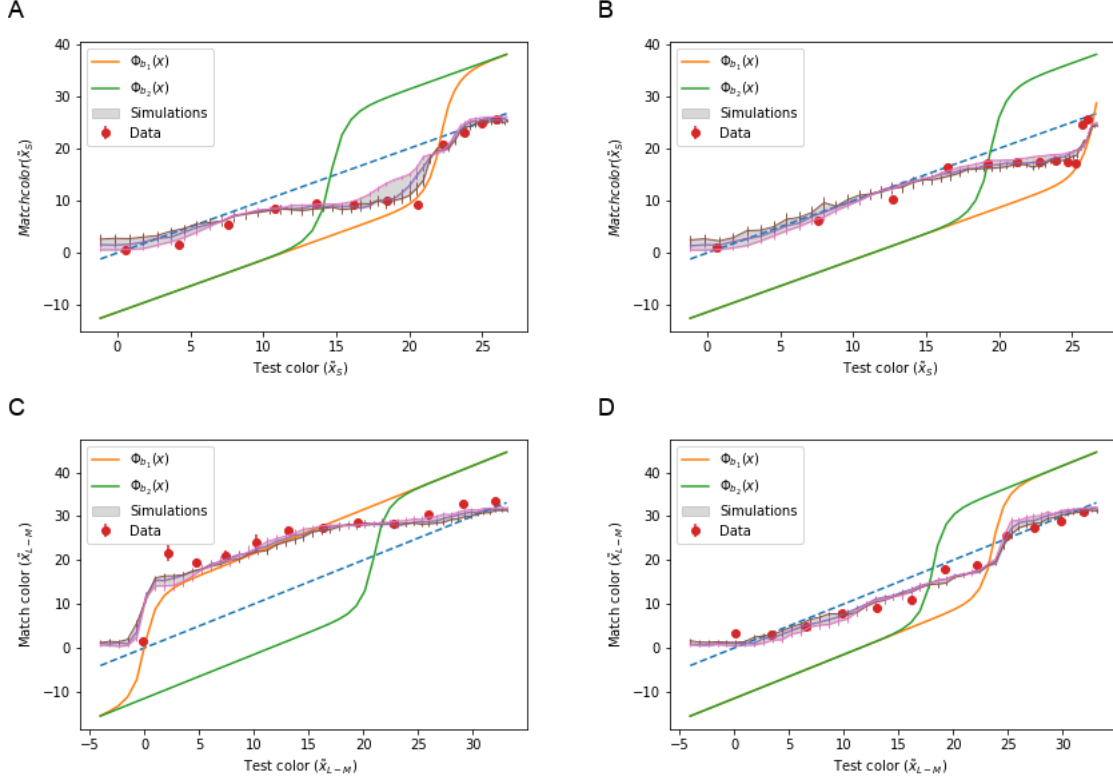


Figure 10: **Comparison between the measured and simulated data in Experiment III.** Matched color x^β as a function of the target color x^α (both axes in the natural coordinates) for observer ST. A and B: Asymmetric matching along the axis \hat{e}^1 . C and D: Asymmetric matching along the axis \hat{e}^2 . In the cone contrast coordinates, the two surrounds were $\mathbf{b}^\alpha = (-0.35, 0)$ and $\mathbf{b}^\beta = (0.25, 0)$ (A), $\mathbf{b}^\alpha = (0, 0)$ and $\mathbf{b}^\beta = (0.9, 0)$ (B); $\mathbf{b}^\alpha = (0, 0)$ and $\mathbf{b}^\beta = (0, -0.1)$ (C), $\mathbf{b}^\alpha = (0, -0.015)$ and $\mathbf{b}^\beta = (0, 0.015)$ (D). Red circles: experimental data. Violet line: Simulated results. Shaded areas: Confidence interval containing the highest 68% of the distribution of simulated results, in the Gaussian approximation. Blue dotted line: identity function, expected in the case in which the surround exerts no influence. Green and orange lines: mappings $\Phi_{\mathbf{b}^\alpha}(x^\alpha)$ and $\Phi_{\mathbf{b}^\beta}(x^\alpha)$ obtained from the fitted values of κ and λ of observer ST, indicating the uniform representatives of $x^\alpha \parallel \mathbf{b}^\alpha$ and $x^\alpha \parallel \mathbf{b}^\beta$, respectively. The perceptual shift induced by the surround becomes relevant in the interval of x^α values for which the two shifts (green and orange curves) are unequal, thereby producing a net unbalance.

4 Conclusions

This paper embraces the conceptual framework first introduced by Resnikoff (1974), and recently reviewed by Provenzi (2020), in which color is understood as a property of classes of equivalence in the space of pairs “stimulus \parallel surround”. This framework was based on the observation that surrounds modify the chromaticity of stimuli. Our starting point was the assumption that, far away from the borders of color space, the perceptual effect of a given surround

on a given stimulus is governed by a universal law. Here, “universal” means that a notion of distance $d(\mathbf{x}_1 \parallel \mathbf{b}_1, \mathbf{x}_2 \parallel \mathbf{b}_2)$ between classes exists, such that

$$\Phi_{\mathbf{b}}(\mathbf{x}) = \gamma_{\mathbf{b} \rightarrow \mathbf{x}} \{t[d(\mathbf{x}, \mathbf{b})]\}, \quad (27)$$

where $\gamma_{\mathbf{b} \rightarrow \mathbf{x}}$ is the geodesic connecting \mathbf{b} and \mathbf{x} obtained from the postulated distance, and t some function that we still need to specify. Equation 27 is a strong assumption. If no symmetries are assumed, $\Phi_{\mathbf{b}}(\mathbf{x})$ can be any transformation $\mathbb{R}^3 \times \mathbb{R}^3 \rightarrow \mathbb{R}^3$. Once Eq. 27 is imposed, the characterization of $\Phi_{\mathbf{b}}(\mathbf{x})$ reduces to the determination of the function $t : \mathbb{R}^+ \rightarrow \mathbb{R}^+$, which is a much simpler object.

If, in addition, the postulated distance derives from a metric tensor with zero curvature, then a system of coordinates exists, here called the *natural coordinates*, in which the perceptual distance is Euclidean. In this coordinate system, all the classes of equivalence have the same shape, and only differ from one another in a rigid translation. The freedom in the shape of $t(d)$ implies that there is freedom in the shape of a single class. Yet, once the manifold corresponding to a single class is known, all others are known too.

In this paper, we tested the hypothesis that the notion of distance required to model chromatic induction through Eq. 27 also governed the perceived similarity of colors in experiments measuring just noticeable differences. If a single notion of distance is involved in a variety of experiments, one may begin to suspect that the space of colors indeed possesses a natural geometry, accessible by many - if not all - the computations implicated in the transformation from input stimuli into behavioral responses. It therefore makes sense to study the geometry of color space, because such geometry is not idiosyncratic to specific tasks: It remains invariant in a variety of paradigms.

Previous work (Krauskopf and Gegenfurtner, 1992; da Fonseca and Samengo, 2016, 2018) had demonstrated that the principal axes of the discrimination ellipsoids were aligned with the coordinate axes, if color was represented in the cone contrast coordinates. Hence, in those coordinates the metric tensor is diagonal, and therefore, has zero curvature. Since the curvature is an invariant property that does not depend on the coordinates, we concluded that the space of colors has zero curvature, and the natural coordinates can be defined for each observer. Importantly, the transformation yielding the natural coordinates was significantly different for different subjects, implying that no unique coordinate system exists, that is perceptually uniform for all trichromatic observers. This finding is in line with the subject-to-subject variability predicted by theoretical derivations in discrimination experiments (da Fonseca and Samengo, 2016), the

population variability in color matching experiments (Stiles and Burch, 1959; Wyszecki and Fielder, 1971; Alfvén and Fairchild, 1997; Fairchild and Heckaman, 2013, 2016; Asano et al., 2016b,a), and experimental studies on chromatic memory (da Fonseca et al., 2019). It is also consistent with the recurrently failed attempts to define a unique coordinate system perceived as perceptually uniform by all observers.

The natural coordinates were only defined with the results of *Experiment I*, and contain no parameters fitted with *Experiments II* and *III*. These coordinates fixate the spacing between uniform representatives. In order to verify whether the homogeneity and isotropy hypothesis are valid, we performed *Experiments II* and *III*. In *Experiment II*, we showed that, in the natural coordinates, the function $t'(|x_i - b_i|)$ was indeed able to describe discrimination experiments in which the stimulus differed from the surround, along both chromatic axes (Fig. 7). Importantly, in the natural coordinates, $|x_i - d_i|$ is the Euclidean distance. Other coordinate systems, instead, yielded data points that could not be well described by a universal law, due to their scatter. These results were restricted to regions of color space in which \mathbf{x} was not far away from \mathbf{b} . Therefore, only the first order Taylor expansion of $t(d)$ could be obtained from *Experiment II*. The restriction was imposed by the limited range of colors that can be produced by a computer monitor. Since discrimination thresholds grow as the surround and the stimulus become farther away from each other, the range of discrimination experiments that can be performed with contrasting surround is limited. This limitation was overcome by *Experiment III*, in which a perceptual match was required from the subject, instead of a discrimination threshold. The results of the match, once again, were revealed to be more universal when displayed in the natural coordinates than in the cone fundamentals (Fig. 9).

The larger range of distances explored by *Experiment III* allowed us to gather evidence for or against different candidate functions $1/t'(d)$. The results of *Experiment II* contradicted Resnikoff’s conjecture of linear classes, and thereby, of thresholds that remained constant as the surround moved away from the stimulus. The hypothesis that follows in simplicity assumes that thresholds grow linearly with d . Yet, this assumption implies that $t(d)$ grows indefinitely in a logarithmic manner, which means that the shift $t(d) - d$ produced by the surround changes sign, a behavior that is somewhat counter intuitive. The simplest next alternative is that after an initial linear trend, thresholds decelerate, and do so sufficiently fast so as to force the perceptual shift $t(d) - d$ to saturate for large distances. One simple way to model this behavior is with thresholds that approached exponentially their upper bound. The comparison between these two options gave a slightly better result for the exponential model. This model was also able to reproduce the temporal sequence of choices of subjects, as illustrated in Fig. 10. We therefore

conclude that the effect of surrounds on the chromaticity of stimuli can be modeled with Eq. 27, with a notion of distance that is individually tailored for each observer, and characterized by the structure of just noticeable distances. The perceptual shift $t(d) - d$ could be well fitted by a simple law that saturates exponentially for large distances.

The universality entailed in Eq. 27 suggests that the same mechanism by which surround b_1 modifies the chromaticity of stimulus x_1 is active when surround b_2 modifies the chromaticity of stimulus x_2 . This mechanism is likely to be implemented by lateral connections in the visual system, or by feedforward connections in which the signals arising from neighboring regions of the visual field converge onto single postsynaptic neuron. If a single physiological mechanism is responsible for the induction observed in different regions of color space, then the natural coordinates are probably the substrate upon which the synaptic processes instantiating induction operate. This hypothesis, if validated by future experiments, would imply that the natural coordinates represent signals that actually exist in the brain, and not just a mathematical construct.

The conclusions supported by our experiments can only be claimed to hold *far away from the borders of color space*, since this is the region that could be tested with our computer monitor. Color space is confined into a cone included inside the positive portion of the 3-dimensional *SML* space, the borders of which are the maximally saturated colors. These colors cannot be generated with LEDs of fairly broad peaks, as the ones comprising computer screens. The existence of a border in color space blatantly contradicts the homogeneity hypothesis. We therefore take special care to limit the validity of our results, since color space cannot be homogeneous near its borders. As a consequence, the exponential model for the repulsive effect produced by surrounds cannot hold near maximally saturated stimuli, since it would push the perceived color outside the boundaries of color space. We therefore conjecture that close to the borders, chromatic induction should diminish. Physiologically, this would mean that when color-representing neurons are firing within a certain specific range (probably their maximal rates) the synaptic mechanisms mediating the chromatic induction produced by surrounds becomes negligible.

Appendix

Table 1: Parameters of the linear and quadratic fits of $x'_i(x_i)$. The reported p -values represent the probability that data as extreme as the ones obtained in the experiment be generated with the fitted model.

J_{11}				J_{22}				
Sub.	α_0	α_1	p -value	Sub.	α_0	α_1	α_2	p -value
NV	25 ± 1	-23 ± 4	0.9962	NV	151 ± 9	-198 ± 39	-2439 ± 1081	0.8826
HW	20 ± 1	-17 ± 3	0.9995	HW	241 ± 12	-55.0 ± 35	-2413 ± 1158	0.9991
ST	18 ± 1	-21 ± 4	0.9933	ST	131 ± 5	-286.0 ± 27	-1324 ± 622	0.4808
IT	19 ± 1	-12 ± 4	0.2271	GM	122 ± 6	-113.0 ± 23	-2393 ± 672	0.5026
YC	16 ± 1	-8 ± 3	0.6555	YS	134 ± 10	-220.0 ± 42	-2770 ± 1065	0.9901

Table 2: Fitted coefficients for Models 1 and 2 (Eqs. 22 and 23) for all measured subjects along the axis \hat{e}^1 .

	Model 1			Model 2		
	γ_0	γ_1	γ_2	γ_0	γ_1	γ_2
NV	0.029 ± 0.004	0.12 ± 0.01	0.43 ± 0.04	0.0021 ± 0.005	0.25 ± 0.02	0.11 ± 0.01
HW	0.0068 ± 0.002	0.064 ± 0.009	0.48 ± 0.02	-0.03 ± 0.003	0.37 ± 0.01	0.092 ± 0.009
ST	0.014 ± 0.004	0.094 ± 0.01	0.23 ± 0.03	-0.0086 ± 0.005	0.17 ± 0.02	0.087 ± 0.009
IT	0.015 ± 0.003	0.038 ± 0.01	0.45 ± 0.03	-0.0072 ± 0.004	0.26 ± 0.02	0.025 ± 0.01
YC	0.015 ± 0.003	0.11 ± 0.01	0.65 ± 0.03	-0.024 ± 0.004	0.39 ± 0.02	0.11 ± 0.01

Table 3: Fitted coefficients for Models 1 and 2 (Eqs. 22 and 23) for all measured subjects along the axis \hat{e}^2 .

	Model 1			Model 2		
	γ_0	γ_1	γ_2	γ_0	γ_1	γ_2
NV	0.0043 ± 0.0008	0.036 ± 0.02	2.1 ± 0.2	$1e - 05 \pm 0.001$	0.26 ± 0.03	0.035 ± 0.02
HW	0.004 ± 0.0003	0.039 ± 0.01	2.3 ± 0.1	-0.00021 ± 0.0004	0.27 ± 0.01	0.039 ± 0.01
ST	0.0032 ± 0.0007	0.049 ± 0.01	2 ± 0.2	-0.0016 ± 0.001	0.24 ± 0.02	0.04 ± 0.01
GM	0.014 ± 0.002	0.1 ± 0.03	2.9 ± 0.4	0.0053 ± 0.002	0.37 ± 0.05	0.077 ± 0.03
YS	0.0034 ± 0.0004	0.096 ± 0.01	2.9 ± 0.2	-0.0018 ± 0.0006	0.32 ± 0.02	0.094 ± 0.01

References

- Alfvin, R. L. and Fairchild, M. D. (1997). Cobserver variability in metameric color matches using color reproduction media. *Color Research & Application*, 22(3):530–539.
- Asano, Y., Fairchild, M. D., and Blondé, L. (2016a). Individual colorimetric observer model. *PLoS ONE*, 11(2):1–19.
- Asano, Y., Fairchild, M. D., Blondé, L., and Morvan, P. (2016b). Color matching experiment

- for highlighting interobserver variability. *Color Research and Application*, 41(15):530–539.
- Chichilnisky, E. J. and Wandell, B. A. (1996). Seeing gray through the ON and OFF pathways. *Visual Neuroscience*, 13(3):591–596.
- Commission Internationale de l’Eclairage (1932). *Proceedings 1931*. Cambridge University Press, Cambridge.
- da Fonseca, M. and Samengo, I. (2016). Derivation of human chromatic discrimination ability from an information-theoretical notion of distance in color space. *Neural Computation*, 28(12):2628–2655.
- da Fonseca, M. and Samengo, I. (2018). Novel perceptually uniform chromatic space. *Neural Computation*, 30(6):1612–1623. PMID: 29566354.
- da Fonseca, M., Vattuone, N., Clavero, F., Echeveste, R., and Samengo, I. (2019). The subjective metric of remembered colors: A fisher-information analysis of the geometry of human chromatic memory. *PLOS ONE*, 14:1–30.
- Derrington, A. M., Krauskopf, J., and Lennie, P. (1984). Chromatic mechanisms in lateral geniculate nucleus of macaque. *Journal of Physiology*, 357(1):241–265.
- Fairchild, M. D. and Heckaman, R. L. (2013). Metameric observers: A monte carlo approach. *Color and Imaging Conference*, 2013(1):185–190.
- Fairchild, M. D. and Heckaman, R. L. (2016). Measuring observer metamerism: The nimeroff approach. *Color Research & Application*, 41(2):115–124.
- Granata, D. and Carnevale, V. (2016). Accurate estimation of the intrinsic dimension using graph distances: Unraveling the geometric complexity of datasets. *Scientific Reports*, 6(1).
- Guild, J. (1932). The colorimetric properties of the spectrum. *Philosophical Transactions of the Royal Society of London A*, 230(681–693):6149–187.
- Jameson, D. and Hurvich, L. M. (1964). Theory of brightness and color contrast in human vision. *Vision Research*, 4(1-2):135–154.
- Kellner, C. J. and Wachtler, T. (2016). Stimulus size dependence of hue changes induced by chromatic surrounds. *Journal of the Optical Society of America*, 33(3):A267–A272.
- Klauke, S. and Wachtler, T. (2015). “tilt” in color space: Hue changes induced by chromatic surrounds. *Journal of Vision*, 15(13):1–11.

- Klauke, S. and Wachtler, T. (2016). Changes in unique hues induced by chromatic surrounds. *Journal of the Optical Society of America*, 33(3):A255–A259.
- Krauskopf, J. and Gegenfurtner, K. (1992). Color discrimination and adaptation. *Vision Research*, 32(11):2165–2175.
- MacAdam, D. L. (1944). On the geometry of color space. *Journal of the Franklin Institute*, 238(5):195–201.
- Mayer, A., Mora, T., Rivoire, O., and Walczak, A. M. (2016). Diversity of immune strategies explained by adaptation to pathogen statistics. *PNAS*, 113(31):8630–8635.
- Provenzi, E. (2020). Geometry of color perception. part 1: structures and metrics of a homogeneous color space. *Journal of Mathematical Neuroscience*, 10(7).
- Resnikoff, H. L. (1974). Differential geometry and color perception. *Journal of Mathematical Biology*, 1:97–131.
- Schrödinger, E. (1920). Grundlinien einer theorie der farbenmetrik im tagessehen. *Annalen der Physik*, 368(21):427–456.
- Silberstein, L. (1943). Investigations on the intrinsic properties of the color domain. *Journal of the Optical Society of America*, 33(1):1–10.
- Spall, J. C. (1998). Implementation of the simultaneous perturbation algorithm for stochastic optimization. *Aerospace and Electronic Systems, IEEE Transactions on, IEEE*, 34:817–823.
- Stiles, W. S. (1946). A modified helmholtz line element in brightness-colour space. *Proceedings of the Physical Society*, 58(1):41–65.
- Stiles, W. S. and Burch, J. M. (1959). Npl colour-matching investigation: final report. *Journal of Modern Optics*, 6(1):1–26.
- Stockman, A. and Sharpe, L. T. (2000). Spectral sensitivities of the middle- and long-wavelength sensitive cones derived from measurements in observers of known genotype. *Vision Research*, 40(13):1711–1737.
- von Helmholtz, H. (1892). Kürzeste linien im farbensystem: Auszug aus einer abhandlung gleichen titels in sitzgsber. der akademie zu berlin. 17. dezember 1891. *Zeitschrift für Psychologie und Physiologie der Sinnesorgane*, 3:108–122.

- Wachtler, T., Albright, T. D., and Sejnowski, T. J. (2001). Nonlocal interactions in color perception: nonlinear processing of chromatic signals from remote inducers. *Vision Research*, 41(12):1535–1546.
- Ware, C. and Cowan, W. B. (1982). Changes in perceived color due to chromatic interactions. *Vision Research*, 22(11):1353–1362.
- Wyszecki, G. and Fielder, G. H. (1971). New color-matching ellipses. *Journal of the Optical Society of America*, 61(9):1135–1152.
- Wyszecki, G. and Stiles, W. S. (2000). *Color Science: Concepts and Methods, Quantitative Data and Formulae*. Wiley Interscience, New York.